

# Photodynamic Therapy of Cancer

Tayyaba Hasan, PhD

Bernhard Ortel, MD

Anne C.E. Moor, PhD

Brian W. Pogue, PhD

## HISTORY

Photodynamic therapy (PDT) is an emerging modality for the treatment of neoplastic and non-neoplastic diseases. It is based on the activation of certain chemicals, called *photosensitizers*, that have been localized in target tissues. Although PDT has been seriously developed for clinical use only relatively recently, the foundations of the concept were laid as early as the beginning of the twentieth century when Raab noted that certain wavelengths of light were lethal to paramecia exposed to acridine and certain other dyes.<sup>1</sup> These observations were followed by the work of von Tappeiner and Jensionek on the use of these dyes topically for the treatment of skin cancer.<sup>2,3</sup> The most explored class of chemical compounds in PDT today, the porphyrins, were investigated by Meyer-Betz as early as 1913 for the accumulation of hematoporphyrin (HP) and its derivatives in rat tumors and PDT effects following systemic administration.<sup>4</sup> The fluorescence from these compounds was further investigated for diagnostic and tumor margin delineation in the late 1940s and 1950s by Figge and colleagues.<sup>5</sup> PDT in its current form can be viewed as having been initiated by the studies of Lipson and Blades, who established that it was an impurity in HP that was the tumor-localizing agent, and not the parent compound.<sup>6</sup> This led to the “synthesis” of hematoporphyrin derivative (HPD), a mixture of porphyrins produced by the acid treatment of HP. The exact chemical composition and structure of this mix remain unclear, although there is general consensus that the active portions consist of porphyrin oligomers with ether and/or ester linkages (Figure 40-1) along with monomeric porphyrins.<sup>7,8</sup> HPD was further developed for laboratory and clinical investigations through the efforts of Dougherty and colleagues in the 1970s and 1980s.<sup>9–11</sup> Tumors in virtually every anatomic site have been treated with PDT, and most are responsive to this therapy to some extent. Although several thousand patients have been treated with PDT for a variety of neoplasms, randomized clinical trials of this modality were initiated only in 1987, using a purified form of HPD, Photofrin (PF).<sup>12,13</sup> These first randomized trials were sponsored by Quadra Logic Technologies, Inc. (now QLT PhotoTherapeutics, Vancouver, Canada) and American Cyanamid Co. (Pearl

River, New York), and compared the efficacy of PDT with that of other forms of therapy for bladder, esophageal, and lung cancers. Within the past 7 years significant progress has been made worldwide in obtaining regulatory approval for a variety of indications. Currently, between Europe and the United States there are five photosensitizing agents approved for the treatment of a variety of diseases. Table 40-1 lists approvals for PDT using PF. Requests for approval for treatment of several other indications, including for early cancers, have been filed in the United States, Canada, Japan, and Europe, and are pending.

## OVERVIEW

Photodynamic therapy is based on the concept (Figure 40-2) that (1) certain photosensitizers can be localized (somewhat preferentially) in neoplastic tissue, and (2) subsequently, these photosensitizers can be activated with the appropriate wavelength (energy) of light to generate active molecular species, such as free radicals and singlet oxygen ( $^1\text{O}_2$ ) that are toxic to cells and tissues. PDT is a binary therapy, and a potential advantage of PDT is its inherent dual selectivity. First, selectivity is achieved by an increased concentration of the photosensitizer in target tissue, and second, the irradiation can be limited to a specified volume. Provided that the photosensitizer is nontoxic, only the irradiated areas will be affected, even if the photosensitizer does bind to normal tissues. Selectivity can be further enhanced by binding photosensitizers to molecular delivery systems that have high affinity for target tissue.<sup>14,15</sup> For photoactivation, the wavelength of light is matched to the electronic absorption spectrum of the photosensitizer so that photons are absorbed by the photosensitizer and the desired photochemistry can occur. Except in special situations, where the lesions being treated are very superficial, the range of activating light is typically between 600 and 900 nm. This is because endogenous molecules, in particular hemoglobin, strongly absorb light below 600 nm and therefore capture most of the incoming photons.<sup>16</sup> The net effect would be the impairment of penetration of the activating light through the tissue. The reason for the 900 nm upper limit is that energetics beyond this wavelength are insufficient to produce  $^1\text{O}_2$ , the activated state of oxygen, perhaps critical for successful PDT.

This chapter provides an overview of the field; excellent reviews and texts on this topic exist.<sup>17–19</sup> In particular, the reader is referred to a review by Dougherty and colleagues.<sup>13</sup> A brief introduction to the relevant photochemistry is given in the next section so that the conceptual basis of PDT may be better understood. While spatial control of illumination, mentioned above, provides specificity of tissue destruction, it can also be a limitation of PDT. Target sites must be accessible to light delivery systems, and issues of light dosimetry need to be addressed.<sup>20,21</sup> In general, the amenability of lasers to fiberoptic coupling makes the task of light delivery to most anatomic sites manageable, although precise dosimetry remains complex and elusive. The effective penetration depth,  $\delta_{\text{eff}}$ , of a given wavelength of light is a function of the optical properties, such as absorption and scatter of the tissue being interrogated. The fluence (light dose) in a tissue is related to the depth,  $d$ , as:  $e^{-d/\delta_{\text{eff}}}$ . Typically, the effective penetration depth is about 2 to 3 mm at 630 nm and increases to 5 to 6 mm at longer wavelengths (700 to 800 nm).<sup>22–24</sup> These values can be altered by manipulating the biologic interactions and physical characteristics of the photosensitizer; however, the relationships are complex. Factors such as self-shielding and photobleaching (self-destruction of the photosensitizer during the PDT) further complicate precise dosimetry, and are discussed further in the section Photodynamic Therapy Dosimetry. In general, photosensitizers with longer absorbing wavelengths and higher molar absorption coefficients at these wavelengths are more effective photodynamic agents.

From a practical point of view, characteristics of the given photosensitizer most relevant to PDT are its concentration,  $c$  (measured on a spectrophotometer), and the extinction coefficient,  $\epsilon$ , which are related by the relationship:  $A = \epsilon c l$ , where  $A$  is the absorption value determined spectrophotometrically, and  $\epsilon$  is the molar extinction coefficient and can be viewed as a measure of efficiency with which the molecule absorbs light of a given wavelength. It is a characteristic of the absorbing chemical species at a specified wavelength under defined conditions, such as in solution or as a solid. In the above equation,  $l$  is the pathlength of light. (In practical terms, this is the width of the cuvette used for determining the absorption values of the photosensitizing agent.)

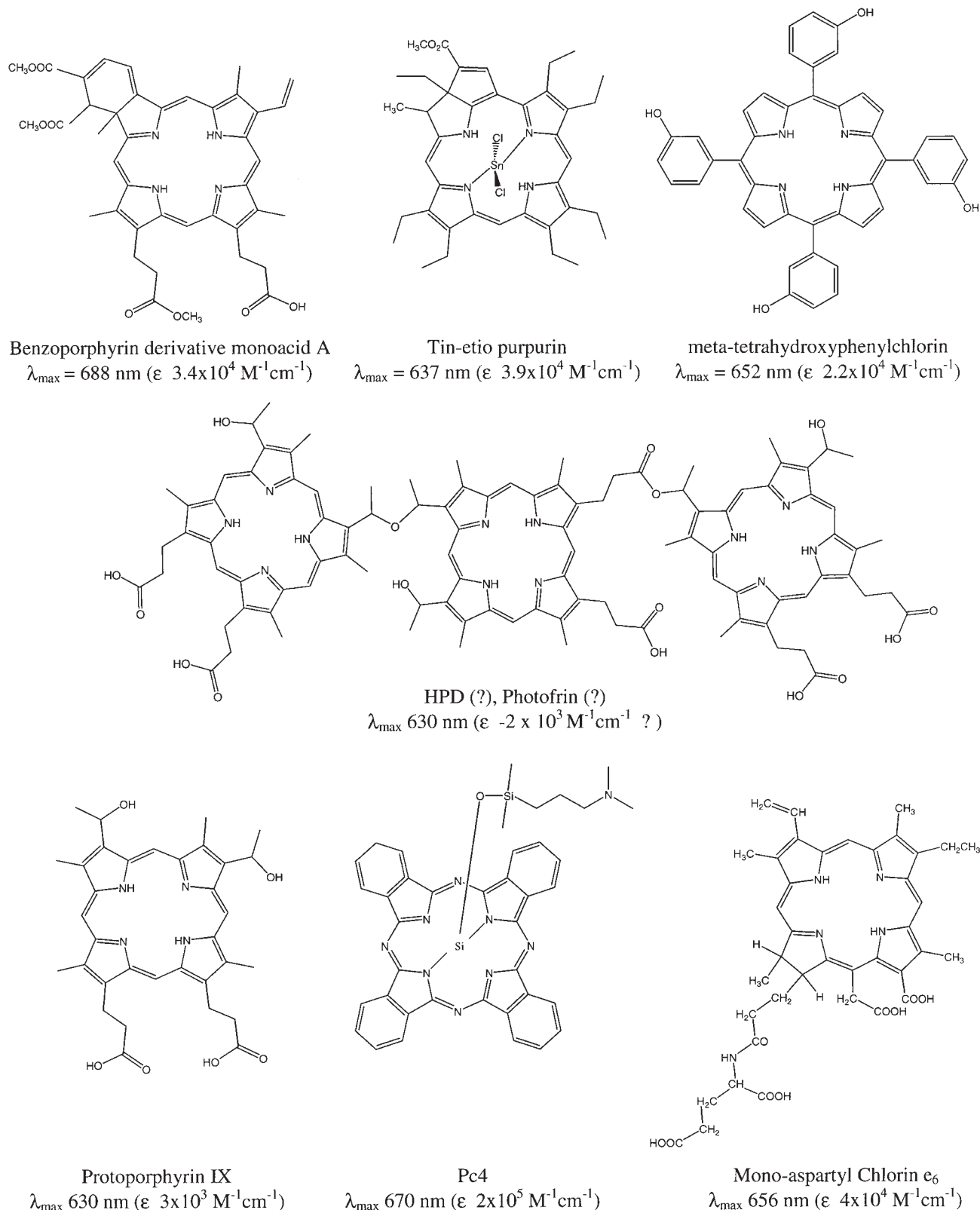


**Figure 40-1** Chemical structures of selected photosensitizers. Underneath the compound name the extinction coefficient  $\epsilon$  at  $\lambda_{\max}$ , the PDT-relevant maximum absorption wavelength, are indicated. Most of the above molecules have their strongest absorption in the 400 nm region (Soret band). This wavelength is generally not useful for clinical applications because of the strong absorption by hemoglobin. In addition, there are other, smaller absorption peaks between 500 nm and 600 nm, some of which are being explored for PDT; however, these are also expected to have strong interference from hemoglobin absorption. For Photofrin (PF)/HPD, indicates the uncertainty of chemical structure for these entities.

### BASICS OF LIGHT AND PDT-RELATED PHOTOCHEMISTRY

Light is a form of electromagnetic radiation that covers a wide range of wavelengths,  $\lambda$ . Between electromagnetic radio wavelengths in the meter

(m) range to gamma rays with wavelengths around  $10^{-11}$  m, visible light relevant to PDT covers the limited range of 4 to  $7 \times 10^{-7}$  m (400 to 700 nm). The energy content ( $E$ ) of light is related to the wavelength of absorption by  $E = h\nu = hc/\lambda$ , where  $h$  is Planck's constant

( $6.63 \times 10^{-34}$  J),  $\nu$  is the frequency,  $c$  is the speed of light in vacuum ( $3.0 \times 10^8$  m/s), and  $\lambda$  is the wavelength. When light is absorbed, the energy of the absorbed photons causes the absorbing molecule to be electronically excited. (Other processes, such as scattering and reflection also

Table 40-1 Overview of Indications for which PDT using Photofrin has been Approved

Country	Indication Statement
Canada	<p><i>Papillary bladder cancer:</i> Posttransurethral resection for recurring superficial papillary bladder cancer as second-line treatment when standard intravesical therapy has failed.</p> <p><i>Esophageal cancer:</i> Reduction of obstruction and palliation of dysphagia for completely or partially obstructing esophageal cancer.</p> <p><i>Endobronchial cancer:</i> Reduction of obstruction and palliation of symptoms for completely or partially obstructing endobronchial non–small-cell lung cancer.</p> <p>Treatment of superficial endobronchial non–small-cell lung cancer when radiotherapy is not indicated.</p>
The Netherlands	<p>Treatment of <i>endobronchial</i> obstruction or endobronchial mucosal lesions by non–small-cell lung cancer or by metastases of other tumor cells to the lung.</p> <p>Treatment of malignant dysphagia caused by tumors within the <i>esophagus</i>.</p>
Japan	<p>The following cancers in which an entire lesion can be observed by endoscopy and laser light delivery is feasible:</p> <ol style="list-style-type: none"> <li>In patients for whom curative therapy, such as surgery, is impossible.</li> <li>In patients whose function of the uterine cervix and lung function need to be retained and there is no therapy except PDT:</li> </ol> <p>Early lung cancer (stages 0 and I); superficial esophageal cancer; superficial gastric cancer, early cervical cancer, and dysplasia.</p>
United States	<p>Palliation for completely or partially obstructing <i>esophageal</i> cancer, where Nd:YAG laser therapy is not possible.</p> <p>Reduction of obstruction and palliation of symptoms for completely or partially obstructing <i>endobronchial</i> non–small-cell lung cancer.</p> <p>Treatment of microinvasive <i>endobronchial</i> non–small-cell lung cancer, where surgery and radiotherapy are not indicated.</p>
France	Treatment of recurrences of non–small-cell <i>bronchial</i> cancer or <i>esophageal</i> cancer which have been previously treated locoregionally.
Germany	Curative treatment for histologically proven non–small-cell <i>endobronchial</i> early carcinomas, where surgery or radiotherapy is not indicated.
United Kingdom	Palliative treatment of obstructing <i>endobronchial</i> non–small-cell lung or obstructing <i>esophageal</i> cancer.
Finland	Obstructive <i>endobronchial</i> non–small-cell lung and obstructive <i>esophageal</i> cancer in patients, in whom conventional treatment is unsuitable.
Iceland	<p>Treatment of superficial <i>endobronchial</i> non–small-cell lung cancer, where surgery or radiotherapy is unsuitable.</p> <p>Palliative treatment of obstructing <i>endobronchial</i> non–small-cell lung and obstructing <i>esophageal</i> cancer.</p>
Denmark	Palliative treatment of obstructing <i>endobronchial</i> non–small-cell lung and of obstructing <i>esophageal</i> cancer.

<sup>a</sup>Courtesy of QLT PhotoTherapeutics Inc, Vancouver, British Columbia, Canada.

occur, as discussed below in the section Photodynamic Therapy). This excitation energy may be converted into heat (kinetic energy) by the collision of the excited molecule with surrounding molecules by radiationless decay. Alternatively, it may be reemitted as fluorescence. The electronic energy levels between which transitions occur by absorption of ultraviolet-visible light ( $\lambda = 200$  to  $700$  nm) may be represented by the simplified energy level diagram presented in Figure 40-3.

The electronic states are represented by the singlet states  $S_0$  to  $S_2$  and the triplet states  $T_1$  and  $T_2$ . (A detailed discussion of the distinction between the singlet and the triplet states is beyond the scope of this chapter. For the purposes of the present discussion, these are two “magnetically”

different excited energized states and arise as a quantum mechanical consequence of electron spin.) With conventional light sources, typical absorption of light by a molecule involves a single photon exciting the molecule to the first excited singlet state  $S_1$ . From this energized state the molecule may initiate photochemistry (depending on the chemical structure) or intersystem cross to an electronically different excited state, the first triplet state  $T_1$ . From  $S_1$ , the excited molecule may also relax back to  $S_0$  by radiationless decay and generate heat or may reemit radiation as fluorescence, which may be used for diagnostic purposes. In general,  $T_1$  is longer lived and chemically more reactive so that the biologically relevant photochemistry is often mediated by this state.  $T_1$  can initiate photochemical reactions

directly, giving rise to reactive free radicals, or transfer its energy to the ground state oxygen molecules ( $^1O_2$ ) to yield excited singlet state oxygen molecules  $^1O_2$ . This excitation to produce  $^1O_2$  requires at least 20 kcal/mol, which places limits on the wavelength of absorption of the photosensitizer. If the energetics are appropriate, photooxidative reactions may occur by  $^1O_2$  mediation. This photodynamic mechanism of cytotoxicity is the generally accepted one for most photosensitizers currently under investigation, although other competing mechanisms exist.  $T_1$  can also potentially relax to  $S_0$  by radiationless decay or by radiative decay as phosphorescence. Under special circumstances (short pulse, high intensities of irradiation), the upper excited states may be populated, and complex photophysical and photochemical processes may originate from these states,<sup>25,26</sup> resulting in increased or decreased phototoxicity, which may include oxygen-independent mechanisms.<sup>26</sup> Studies into radical-mediated photosensitizers and photosensitizers that are specifically activated by multiple-photon absorption mechanisms is ongoing.

## PHOTOSENSITIZERS

There are a fairly large number of photosensitizers under preclinical development at the present time. No attempt is made in this chapter to cover all of them comprehensively. The reader is referred to the many existing reviews.<sup>13,17,27–30</sup> Only the few photosensitizers that are in advanced stages of clinical development in the United States are discussed.

**ANIONIC LIPOPHILIC PHOTOSENSITIZERS** By far the majority of clinical experience in PDT has been with PF, and for a long time, preclinical studies were dominated by investigations using some form of HPD. Clinical results with PF are promising, and this photosensitizer has received regulatory approval in a number of countries. However, it is plagued by prolonged cutaneous phototoxicity, which can last up to 4 to 6 weeks. In addition, it is poorly characterized chemically and has relatively low absorption in the wave-

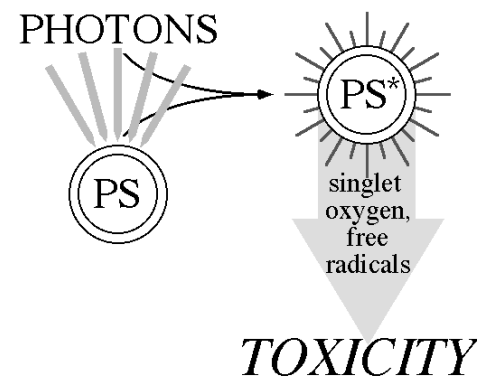


**Figure 40-2** A simplified representation of events in photodynamic action. Appropriate energy photons are absorbed by light-activable molecules, photosensitizers (PS). Activated PS (PS\*) leads to the formation of reactive molecular species that cause cytotoxicity.

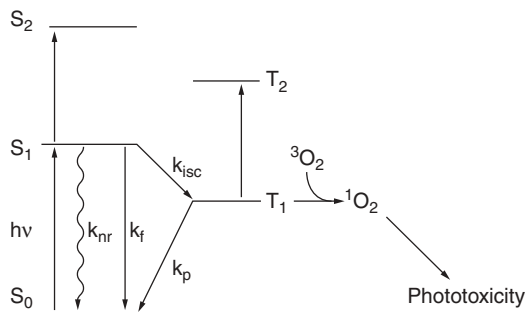


**Figure 40-3** A simplified energy level diagram for the photoexcitation of a molecule.  $S_0$ ,  $S_1$ , and  $S_2$  represent singlet electronic states of the molecule. Absorption of a photon (depicted by  $h\nu$ ) results in the excitation of the absorbing molecule from the ground singlet state,  $S_0$ , to the first excited singlet state,  $S_1$ . Photochemistry may occur from  $S_1$  directly or from the first triplet excited state,  $T_1$ , which is generated after intersystem crossing. The molecule can relax back to the ground state  $S_0$  from either  $S_1$  or  $T_1$  radiatively or nonradiatively.  $k_{nr}$ ,  $k_{isc}$ ,  $k_f$ , and  $k_p$  represent rate constants for nonradiative decay, intersystem crossing, fluorescence, and phosphorescence, respectively. In general, with conventional light sources, only  $S_1$  and  $T_1$  are populated. With high-intensity, pulsed irradiation, or with two-wavelength excitation, the upper excited states, such as  $S_2$  and  $T_2$ , may also be populated, giving rise to different photochemistry.

length region of therapeutic interest (600 to 900 nm, see Figure 40-1). These factors, plus an increase in the clinical applications of PDT, have stimulated research in the synthesis and testing of new, non-PF photosensitizers<sup>28-31</sup> and in improved methods of localizing them.<sup>31</sup> A significant number of new photosensitizers have been synthesized and show promise in their initial testing. In addition to avoiding nonspecific phototoxicity, their development has been motivated by the possibility of treating larger tumor volumes because of the greater penetration depth of longer wavelengths of light. Therefore, the properties that were aimed for in the development of these sensitizers were improved selectivity, longer wavelengths of light absorption, and increased extinction coefficient (molar absorptivity) at these wavelengths. Currently, there may be more than 30 photosensitizers in laboratory investigations, all of which are tetrapyrrole compounds. Table 40-2 summarizes selected compounds that are being tested preclinically and clinically and Figure 40-1 presents the chemical structures with therapeutically relevant photophysical properties for some of those compounds.

In general, these newer compounds show somewhat improved selectivity for tumor over normal tissue as compared to PF, and consequently have reduced associated cutaneous phototoxicity. For some, the pharmacokinetics are reasonably rapid with plasma half-lives that are often biphasic, with values ranging from a few hours to a few days. They also have superior photochemical properties in terms of the absorption at longer wavelengths and corresponding extinction coefficients. For example, the chlorins have red-shifted absorption spectra ( $\lambda_{max}$  650 to 670 nm),

as compared with 630 nm for PF<sup>32-34</sup> and extinction coefficients in the  $3$  to  $5 \times 10^4 \text{ M}^{-1} \text{ cm}^{-1}$  range, as compared with the estimated values of up to  $2 \times 10^3 \text{ M}^{-1} \text{ cm}^{-1}$  for PF. Of the newer photosensitizers, the most developed is benzoporphyrin derivative monoacid A (BPD-MA).<sup>35,36</sup> For clinical applications, this molecule is liposomally formulated and has good absorbance at longer wavelengths (see Figure 40-1). BPD-MA has shown encouraging results in the Phases I and II clinical studies for the treatment of cutaneous malignancies (both primary and metastatic lesions). However, because of its effectiveness in the obliteration of neovessels, this compound is being aggressively developed by QLT Phototherapeutics and Ciba-Vision as a first-line treatment for age-related macular degeneration (AMD) of the eye.<sup>37-40</sup> This direction was stimulated by a series of preclinical studies,<sup>37</sup> in which intraocular tumors implanted in rabbit eyes were used as a model for neovascularization. These studies showed that the very efficient destruction of these tumors could be attributed primarily to the destruction of the tumor neovascularization; the established choroidal vessels remained largely intact. Currently, the use of BPD-MA in the liposomal formulation called verteporfin, is used in Visudyne therapy marketed by Novartis Ophthalmics, for the treatment of classic subfoveal neovascularization (CNV) caused by AMD. This treatment was approved in the United States by the Food and Drug Administration (FDA) in 2001 following promising Phases I and II clinical trials demonstrating that the treatment could slow the loss of vision in patients with CNV, pathologic myopia, and ocular histoplasmosis.<sup>41</sup> Currently Visudyne treatment is approved in 60 countries, and has rapidly become a major commercial success for PDT treatment, which will likely become approved for other indications in ophthalmology in the near future. At the time of the writing of this chapter, BPD-MA (Visudyne) is commercially available in 65 countries for the treatment of predominantly classic subfoveal CNV caused by AMD. It is additionally approved in 44 countries, including the European Union (EU),

United States, and Canada, for the treatment of subfoveal CNV caused by pathologic myopia (severe nearsightedness). In some countries Visudyne is also approved for presumed ocular histoplasmosis or other macular diseases. For the occult form of subfoveal CNV, Visudyne is approved in the EU and United States. Clinical trials are ongoing to achieve approval for treatment of CNV with chlorin- and phthalocyanine-based photosensitizers produced by other companies, perhaps expanding the variety of compounds and mechanisms of action that will be used in AMD therapy.

**CATIONIC PHOTOSENSITIZERS** A different group of photosensitizers that merits a brief mention are the cationic photosensitizers. In contrast to the porphyrins, which derive their PDT effect in large part via destruction of the tumor vasculature, cationic photosensitizers are suggested to be cellularly localized molecules and to act at the tumor cell level. It is believed that the basis for their preferential accumulation in tumor tissue is that the electrical potential across the mitochondrial membrane in tumor cells is much steeper than in normal cells.<sup>42</sup> This steep gradient leads to a high accumulation in tumor cells of compounds with a delocalized positive charge. The best developed of the series are the benzophenothiazinium dyes.<sup>43,44</sup> In systematic investigations of these dyes, Cincotta and colleagues showed high cure rates in two animal models of sarcoma, using the cationic photosensitizer 5-ethylamino-9-diethylamino-benzo[a]phenothiazinium chloride activated with 652-nm irradiation.<sup>44</sup> Minimal damage to surrounding and overlying skin tissue was observed, pointing to the selectivity of this compound. Histologic and fluorescein dye exclusion data indicated minimal damage to the irradiated vasculature within and surrounding the tumor. Cellular uptake of these compounds appears to occur rapidly, within seconds. In an attempt to combine vascular and cellular effects, a benzophenothiazinium sensitizer and BPD-MA were used in PDT of EMT-6 tumors in Balb/c mice. The treatment produced a synergistic

**Table 40-2 Selected Non-PF Photosensitizers and Experimental Clinical Studies<sup>a</sup>**

Photosensitizer	Cutaneous Lesions	Early Upper <sup>¶</sup> Aerodigestive Esophagus Bronchus	Gynecology (Endometrial, Cervical, Vulvar)	Age-Related Macular Degeneration	Other Applications
ALA-PpIX	X	X	X		X
BPD-MA	X		X	X	
Porphycenes	X				
MACE	X				
Tin-etio-purpurin	X		X	X	
mTHPC	X	X	X		
NPc6				X	
Pc4	X				
Lutetium texaphyrin	X		X		

ALA-PpIX =  $\delta$ -aminolevulinic acid-induced protoporphyrin IX; BPD-MA = benzoporphyrin derivative monoacid A; MACE = mono-aspartyl chlorin e<sub>6</sub>; mTHPC = meta-tetrahydroxyphenylchlorin; Pc4 = a silicon phthalocyanine.

<sup>a</sup>This list is not meant to be exhaustive. Because PDT is rapidly expanding, there are likely to be more applications than listed here.

effect, compared with the single treatments.<sup>45</sup> By using the iodinated form of the cationic photosensitizer, it was shown that the antitumor effect was mediated by both T cells and natural killer (NK) cells, indicating that PDT can elicit antitumor protective immunity.<sup>46</sup> These preclinical studies may be useful in various clinical settings and are currently under development.

**$\delta$ -AMINOLEVULINIC ACID-BASED PDT** Typically, in the application of PDT, presynthesized sensitizers are administered, followed by a delay period that, depending on the photosensitizer, may vary from 30 min to 7 days. The rationale for the shorter times is that the photosensitizer is largely in the bloodstream during irradiation so that a shut-down of the tumor vasculature may be achieved. At longer delays, the photosensitizer is expected to be cleared from normal tissues, and there is some preferential retention in tumor tissue; light activation then leads to photocytotoxicity, as already discussed (see Figures 40-1 and 40-2).

Recently, there has been much interest in a different approach to PDT where, instead of a photosensitizer being administered in a synthetic form, a precursor is administered, and the photosensitizer is synthesized *in situ* in tumors.<sup>47</sup> This is the case with  $\delta$ -aminolevulinic acid (ALA). ALA is a naturally occurring precursor in the biosynthetic pathway for heme production, as shown in Figure 40-4. The last step in the biosynthetic route involves conversion of protoporphyrin IX (PpIX), a photosensitizing species, to heme (a nonphotosensitizing agent). Under physiologic conditions, cellular heme synthesis is regulated in a negative feedback control of the enzyme ALA synthase by free heme. ALA synthase then becomes the rate-limiting step. Figure 40-4 depicts the heme pathway under normal conditions and under exogenous ALA exposure. When exogenous ALA is added, the control mechanism is bypassed, and downstream metabolites are synthesized in excess. Under these conditions, ferrochelatase, which catalyzes iron insertion into PpIX, becomes the rate-limiting enzyme. Following the addition of exogenous ALA, the low physiologic rate of iron insertion by ferrochelatase is unable to compensate for the excess PpIX that is formed. PpIX, therefore, accumulates in cells and renders them photosensitive.

ALA-based PDT has been used primarily in the treatment of nonmelanoma skin cancers because of the skin's accessibility to light treatment and the availability of a preparation of ALA for topical use.<sup>47</sup> In this indication, ALA-based PDT compares well with other forms of PDT, and likewise has favorable patient acceptance because of excellent cosmetic results.<sup>48</sup> While cutaneous lesions are easily sensitized with topical preparations, other tumor locations need systemic sensitization by ingestion of ALA doses up to 60 mg/kg body weight. For PDT of oral cancer, systemic ALA photosensitization has been successful.<sup>49,50</sup> Patients with Barrett's esophagus, precancerous dysplasia and early esophageal carcinomas are

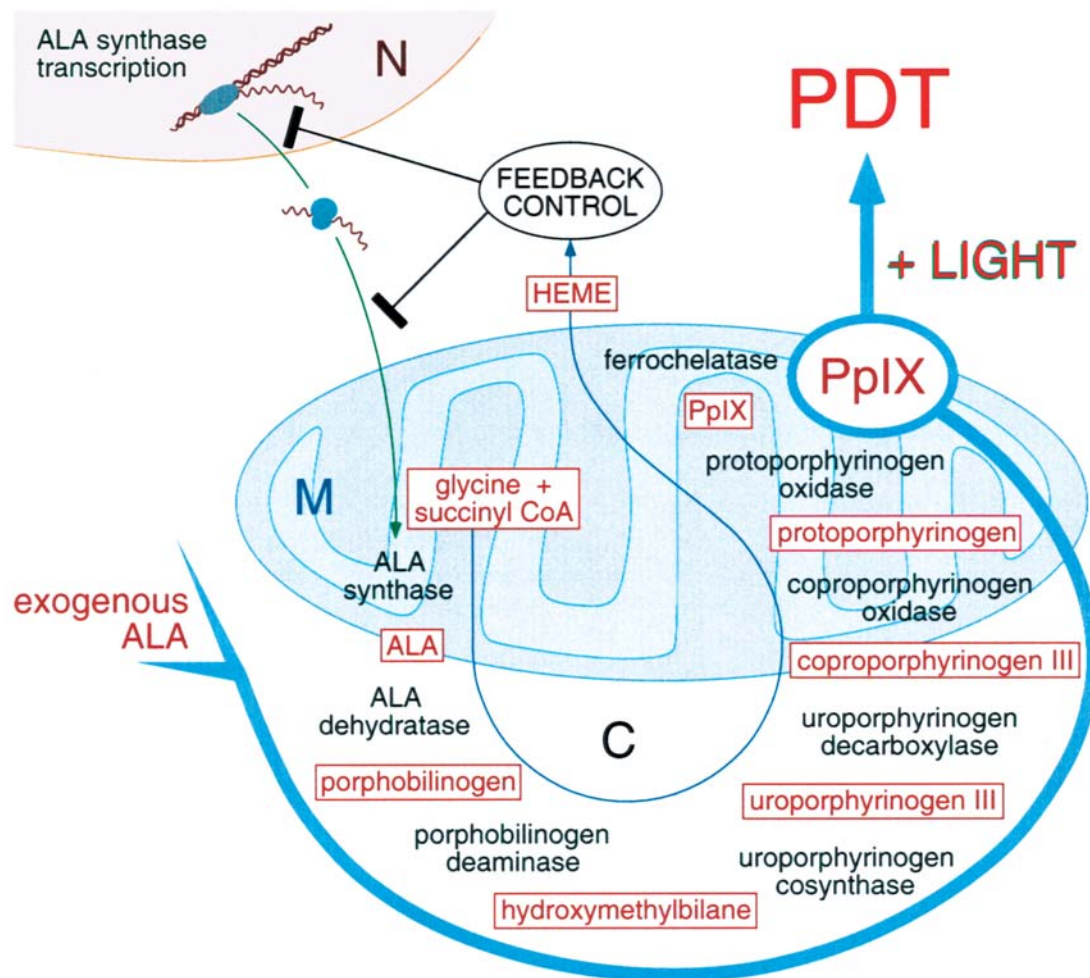


**Figure 40-4** The biosynthetic pathway for the production of heme. The enzymes and metabolites are located in the mitochondria (M) and the cytosol (C). Heme negatively regulates ALA synthase at several points, two of which are shown in the figure. Exogenous ALA induces excess formation of heme precursors, including PpIX that can be used for photosensitization (depicted by the thick line). (N) nucleus, where transcriptional control occurs. (Four-color version of figure on CD-ROM)

being efficiently treated with oral ALA-based PDT, although the current data suggests that the treatment is most successful in smaller tumor regions.<sup>51,52</sup> In this specific indication, selective PpIX accumulation in the epithelium seems to help prevent strictures that are a complication of PDT with PF.<sup>53,54</sup> Clinical trials are ongoing to improve the overall efficacy of Barrett's treatment, examining variations in drug delivery and light dosimetry to optimize treatment conditions.

Although therapeutic indications are expanding, the use of ALA-induced PpIX (ALA-PpIX) has gained much interest in diagnostics. PpIX fluorescence is being developed for the detection of early malignancies, carcinomas *in situ*, and cancer precursor lesions. By minimally invasive diagnostic procedures, accessible organs, such as the bladder,<sup>55-57</sup> oral cavity,<sup>58,59</sup> lungs,<sup>60</sup> upper and lower gastrointestinal tract,<sup>61,62</sup> and cervix,<sup>63,64</sup> to name a few, are being viewed with optical devices, and ALA-PpIX fluorescence is used to detect suspicious areas for guided biopsy and therapy. In urology, ALA-PpIX is used for the early diagnosis of urothelial dysplasia and carcinoma. Figure 40-5 shows an image from a cystoscopic examination of the bladder. In this case, the ALA is adminis-

tered locally by instillation and remains for about 2 h in the bladder. Subsequently, the bladder wall is examined by using a modified cystoscope that allows regular illumination and blue-light excitation for observation of porphyrin fluorescence. With white light, the lesion can be barely distinguished, while blue light-induced ALA-PpIX fluorescence clearly demonstrates the outline of the neoplasia. In larger patient groups, this use of ALA significantly enhanced the cystoscopic detection of malignant and dysplastic lesions,<sup>56</sup> and in the application of imaging following surgical resection it has been shown to be a useful "second-look" tool to find remaining dysplastic tissues, thereby significantly reducing the local recurrence rate following surgery.<sup>57</sup> ALA-PpIX fluorescence is also useful for determining tumor margins. In a similar manner, during brain surgery ALA-PpIX fluorescence-guided resection of malignant gliomas reportedly results in prolonged patient survival.<sup>65-67</sup>

In contrast to most tetrapyrrole photosensitizers, ALA-PpIX localizes in cells (where it is synthesized) rather than in the tumor vasculature.<sup>48,68</sup> The effects of exogenous ALA cannot be imitated by administration of presynthesized PpIX.<sup>17</sup>

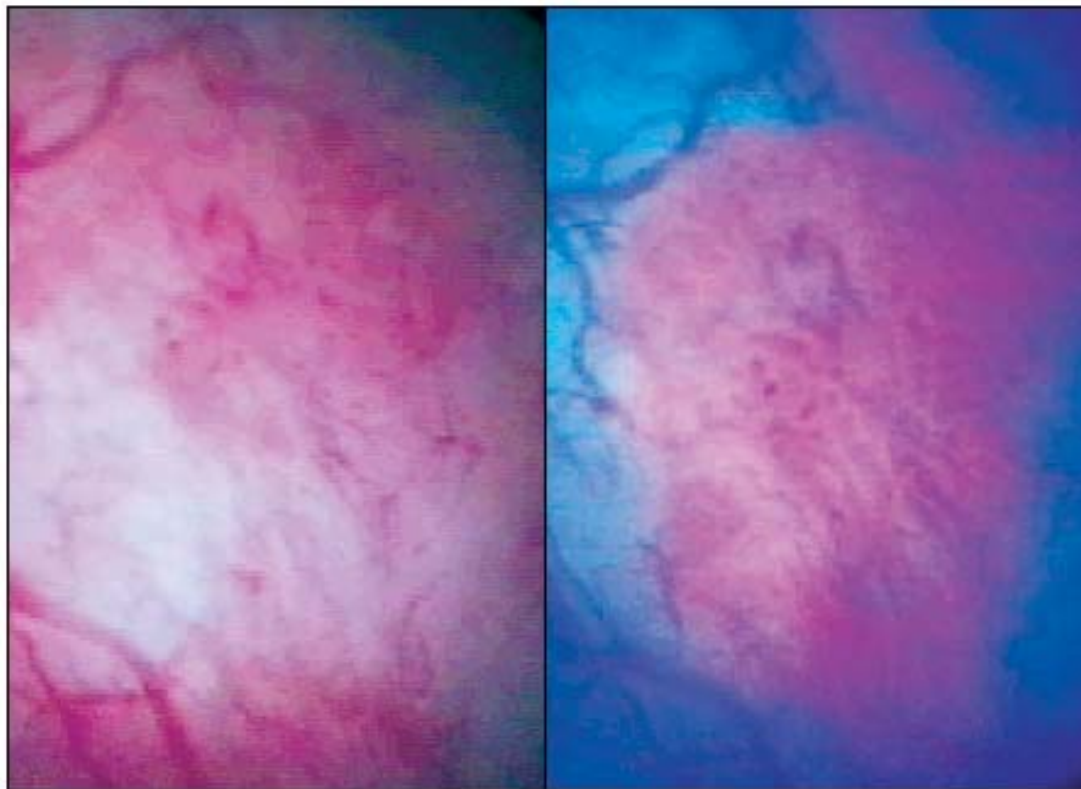


**Figure 40-5** Fluorescence diagnosis of urothelial dysplasia in the bladder clinically. Cystoscopic images of the bladder wall of patients after instillation of 50 mL of a 3% ALA solution for 2 h for the induction of PpIX formation. The conventional white-light image to the left did not show the extent of the neoplastic lesion, which is revealed by the pink PpIX fluorescence under blue illumination of the same view on the right. Images courtesy of Reinhold Boumgartner, PhD. (Four-color version of figure on CD-ROM)

ALA<sup>69</sup> and ALA-PpIX<sup>70</sup> are rapidly cleared from the system, which results in an acceptably short period (< 24 h) of cutaneous photosensitivity. This is viewed as an advantage over some of the other photosensitizers where light protection may be required for several weeks.

Concurrent with clinical studies in humans, there has been much experimental work in cell culture and in animals aimed at understanding the mechanisms of ALA-based PDT, in order to develop strategies for more effective clinical response.<sup>71–73</sup> At present, our knowledge of the mechanisms involved in ALA-based PDT is limited. For example, the reason for preferential ALA uptake and conversion by tumors and dysplastic tissue is not clear. No matter how good the delivery of ALA may be, the formation of PpIX requires the activity of several enzymes (see Figure 40-4), the manipulation of which presents an opportunity to improve PDT. At this point, the relative importance of various enzymes seem dependent on the tumor/tissue type. For example, it has been proposed that some tumors contain lower levels of ferrochelatase, resulting in enhanced ALA-PpIX accumulation. A reduced availability of iron reduces heme formation by ferrochelatase, and iron metabolism has been shown to play a role in ALA-based PDT.<sup>74,75</sup> There is some indication that porphobilinogen deaminase is another important enzyme and is upregulated under exogenous ALA stimulation.<sup>76</sup>

Proliferating tissues and malignant cells are generally considered more efficient in ALA-PpIX formation,<sup>72</sup> but recently an inverse relationship in which growth arrest was associated with differentiation was documented.<sup>77</sup> In differentiating (growth-arrested) primary keratinocytes, an increased production of ALA-PpIX was accompanied by an upregulation of coproporphyrinogen oxidase at the mRNA level,<sup>78</sup> compared with their nondifferentiated (proliferating) counterparts. The increased cellular PpIX content enhanced PDT efficacy. The same increase of ALA-PpIX formation with cellular differentiation was also found in other cellular models of differentiation,<sup>78,79</sup> including a human prostate cancer cell line (LNCaP). In the latter, differentiation was induced with a synthetic androgen receptor ligand, which resulted in an up to tenfold enhanced ALA-PpIX production and led to enhanced photocytotoxicity. Figure 40-6 shows a dramatic increase in the PpIX content differentiated in LNCaP cells by confocal scanning fluorescence microscopy after 4 h of ALA exposure. Quantification showed a greater than tenfold enhancement in the PpIX content of the differentiated LNCaP cells over the undifferentiated ones, along with an increase in PDT responsiveness. These findings suggest a potential for a new combined therapeutic regimen, where induction of differentiation precedes ALA-based PDT and makes tumors more susceptible to photosensitization.

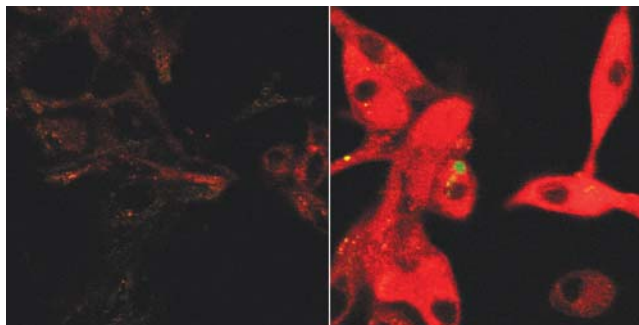
To improve the penetration of topically applied ALA and improve selectivity, the development of ALA esters is being investigated. The cells take these up, and esterase hydrolysis yields ALA that enters the heme pathway and induces PpIX production.<sup>80</sup> ALA esters have different molecular properties, which alter pharmacokinetics and bioavailability. The data indicates that the altered properties further improve the diagnostic and therapeutic potential significantly beyond what is achieved with ALA-based PDT.<sup>81,82</sup> The rapid degradation of the ester compounds in the blood limits the penetration to immediately near the site of topical application, thereby limiting PpIX production in surrounding normal tissues, and improving the overall tumor to normal tissue selectivity. Several of these esters are in preclinical and clinical investigations.<sup>81–86</sup>

### PHOTOSENSITIZER TRANSPORT AND DISTRIBUTION

The accumulation of a photosensitizer in neoplastic tissue relative to normal tissue depends on the photosensitizer, the normal tissue being considered, and, in the laboratory situation, the animal tumor model being investigated. The reason for the preferential accumulation in tumor tissue compared with certain normal tissues not belonging to the reticuloendothelial system is not clearly understood. It may be a result of the greater proliferative rates of neoplastic cells, poorer lymphatic drainage, leaky vasculature, or some more specific interaction between the photosensitizer and marker molecules on neoplastic cells. Other factors, such as the secretion of vascular endothelial growth factors, may be important in photosensitizer accumulation in tumor tissue.<sup>87</sup> Immediate tissue effects following photodynamic treatment with porphyrins under the most frequently used protocols suggest that the tumor vasculature is a primary early target.<sup>88–90</sup> In the typical preclinical and clinical protocols, most porphyrin photosensitizers appear to be localized in the tumor vasculature.<sup>88,91</sup> These observations suggest a possible specific interaction of the photosensitizers with tumor vasculature; however, there is also considerable evidence that at longer times after application of the photosensitizer, the treatment effects becomes distinctly less vascular.<sup>92</sup> This interplay between vascular and cellular causes of tumor destruction is discussed further in the next section.

One suggested specific interaction has been the low-density lipoprotein (LDL) receptor–photosensitizer interaction leading to increased photosensitizer concentrations in neoplastic tissue. It is suggested that LDL receptors on tumor cells and on tumor vascular endothelial cells play a role in the uptake of photosensitizers, a role that may be direct or receptor mediated. This is attributed to increased expression of LDL receptors in malignant cells and neovascular endothelial cells. The increased expression of LDL receptors in malignant cells may be caused by either an increased rate of cell proliferation or an increased rate of membrane turnover without proliferation. The suggestion is that two classes

**Figure 40-6** Confocal laser scanning fluorescence micrographs showing increased ALA-induced PpIX levels with cellular differentiation. Human prostate cancer cell line LNCaP was exposed to 0.3 mmol/L ALA for 4 h. The red fluorescence stems from PpIX synthesized within the cells. The cells on the left were grown in androgen-free medium. The cells on the right were pretreated for 4 days with the synthetic androgen-receptor ligand R1881, which acts as a differentiating agent. (Four-color version of figure on CD-ROM)



of binding sites exist on lipoproteins for porphyrins probably located in the apoprotein matrix and the lipid core.<sup>93,94</sup> LDL-associated photosensitizer is then targeted to cellular or vascular components of the tumor. These conclusions are based largely on photosensitizer pharmacokinetics and tissue distribution studies with a number of photosensitizers, primarily PF, the most frequently used photosensitizer clinically.

These pharmacokinetic investigations led to the general agreement that PF binds to both albumin and lipoproteins. Initially, the binding occurs almost equally to LDL and to high-density lipoproteins (HDLs).<sup>93</sup> At longer time periods, the binding occurs almost exclusively to HDL, with a small fraction being associated with LDL. The thought is that association with LDL carries the photosensitizer to tumor tissue. A correlation between LDL receptor level (in neoplastic and reticuloendothelial cells) and PF distribution has been suggested.<sup>95</sup> An approximate generalization based on such pharmacokinetic studies with a variety of photosensitizers is that hydrophobic dyes are associated with lipoproteins, while their hydrophilic counterparts bind preferentially to other serum proteins, such as albumin.<sup>96</sup> The significance of this hypothesis was tested in a study by Kongshaug and colleagues for the distribution of porphyrins and chlorines with different tumor-localizing ability among human plasma proteins.<sup>97,98</sup> The goal of these studies was to ascertain whether there was any correlation between the lipophilicity and LDL-binding capability and tumor-localizing ability. The conclusion was that increasing lipophilicity did, in general, increase binding to LDL (Table 40-3). Some exceptions were noted. Protoporphyrin (PP) and HP bind to a similar extent to heavy proteins, even though HP is significantly more polar than PP. Similarly, tetraphenylporphine axial disulfonate (TPPS<sub>2a</sub>) binds more extensively to LDL than does the monosulfonated TPPS<sub>1</sub>, which is significantly less polar. This anomalous behavior was attributed to the asymmetric charge distribution on TPPS<sub>2a</sub>, which may cause a high affinity for a lipid-water interface. The asymmetry of TPPS<sub>2a</sub> was previously invoked by Kessel and colleagues as an explanation for their observation that the TPPS<sub>2a</sub> has a higher uptake in cells than does TPPS<sub>1</sub>.<sup>99</sup> Additionally, the extent of binding to LDL did not always correlate with tumor localization. It was noted that HP has a higher relative affinity for LDL than does TPPS<sub>4</sub> and that PP has an even

higher affinity, but HP and PP are generally considered inefficient tumor localizers.<sup>100</sup> PF has a relative affinity for LDL between that of HP and that of PP, but is a good tumor localizer. Similarly, TPPS<sub>4</sub>, with a very low affinity for LDL and a relatively high affinity for heavy proteins, is an efficient selective tumor localizer.<sup>100-102</sup>

In studies using both murine models and human plasma, Kessel and colleagues<sup>103,104</sup> demonstrated that a relatively hydrophilic compound *N*-aspartyl chlorin e6 (NPe6) bound largely to albumin and HDL, and that only 1% to 2% bound to LDL. Insofar as successful destruction of mouse tumors has been reported with NPe6,<sup>105,106</sup> it is clear that non-LDL modes of photosensitizer localization in tumor tissue are operative and important. In the case of NPe6, tumor destruction is believed to be dominated by vascular shutdown.<sup>106</sup> Optimal tumor necrosis was not obtained when tumors were irradiated at times of maximal intratumoral photosensitizer concentration. Factors such as binding to other proteins, aggregation properties, polarity, pH effects, and the chemical nature of side-group photosensitizer and metal ligands are probably equally important determinants of association with lipoproteins. Also, the photosensitizers in serum are probably in a dynamic state as they are transferred between various protein fractions within the same serum.

The generalization that hydrophobic compounds are transported in vivo via lipoproteins appears to be true for the photosensitizer family of benzoporphyrin derivatives (BPDs) in experimental clinical use. These compounds absorb strongly around 690 nm and are composed of four structural analogs. The ring A monoacid analog (BPD-MA) has been the most developed of the series. Preclinical studies of BPD-MA biodistribution showed that the majority of the BPD-MA (55%) is associated with HDL, 15% with LDL, 6% with albumin, and 3% with very-low-density lipoprotein (VLDL).<sup>107,108</sup> On the basis of these preclinical studies, a liposomal preparation of BPD-MA has been used in various Phase I to Phase III clinical trials for a variety of pathologies,<sup>109,110</sup> with high clinical success in the treatment of AMD, as described earlier.

### BIOLOGIC MECHANISMS OF PDT

**CELLULAR MECHANISMS** The cellular mechanisms involved in PDT have been studied exten-

sively, and as with other modalities, these depend on the specific conditions under which they are investigated. These mechanisms have been reviewed recently,<sup>13,111</sup> and only the more recent developments are discussed below.

In complex environments, such as cells and tissues, the subcellular localization of the photosensitizer is important for effective photochemistry to occur. For electron transfer reactions, an interaction between the excited sensitizer and a donor or acceptor molecule is necessary; if these happen to be cellular targets, photobiologic effects occur. Energy transfer reactions involving <sup>1</sup>O<sub>2</sub> require close proximity of sensitizer and target, because <sup>1</sup>O<sub>2</sub> can diffuse only about 20 nm in cells, a result of efficient quenching in biologic environments.<sup>112</sup> Therefore, the cellular structures close to both a high sensitizer and a high oxygen concentration will be preferentially damaged on illumination. Subcellular localization is mainly dependent on the physicochemical properties of the photosensitizer but may be altered by using specific delivery vehicles (see section Photodynamic Therapy with Targeted Molecular Delivery System) and modifying the status of the cell itself.<sup>78</sup> In a series of studies, Kessel and coworkers showed that sensitizers that localize in mitochondria are very rapid inducers of apoptosis, in contrast to photosensitizers localized in lysosomes and plasma membranes.<sup>113-115</sup> Figure 40-7 shows the primarily mitochondrial localization of BPD-MA, which, on photosensitization, induces apoptosis efficiently (see section Photodynamic Therapy with Targeted Molecular Delivery System). For lysosomal photosensitizers, the mode of cell death is dominated by necrosis, possibly because of the release of lysosomal enzymes and other toxic moieties. There is, however, a possibility of lysosomally localized photosensitizer relocating to mitochondria within the first few seconds of illumination, where they may be considerably more phototoxic.<sup>116</sup>

Apoptosis induction by photosensitizers primarily localized to the mitochondria is an

**Table 40-3** Distribution of Porphyrins among Human Plasma Proteins

Porphyrin	Retention time (min) RPC18 <sup>a</sup>	Distribution (%)		
		LDL	HDL	Heavy Proteins
HP	~3	10	55	35
PF	3.6-20	16	70	14
PP	18	22	41	37
TPPS <sub>4</sub>	0.05	1-2	18	80
TPPS <sub>3</sub>	0.35	6	68	26
TPPS <sub>2o</sub>	3.95	7	74	19
TPPS <sub>2a</sub>	10.1	36	55	9
TPPS <sub>1</sub>	20.0	30	60	1

HDL = high-density lipoprotein; HP = hematoporphyrin; LDL = low-density lipoprotein; PF = Photofrin; PP = protoporphyrin; TPPS = tetraphenyl porphine.

<sup>a</sup>HPLC (high-pressure liquid chromatography) retention time is a measure of hydrophobicity.

Data from Kongshaug et al.<sup>97</sup>

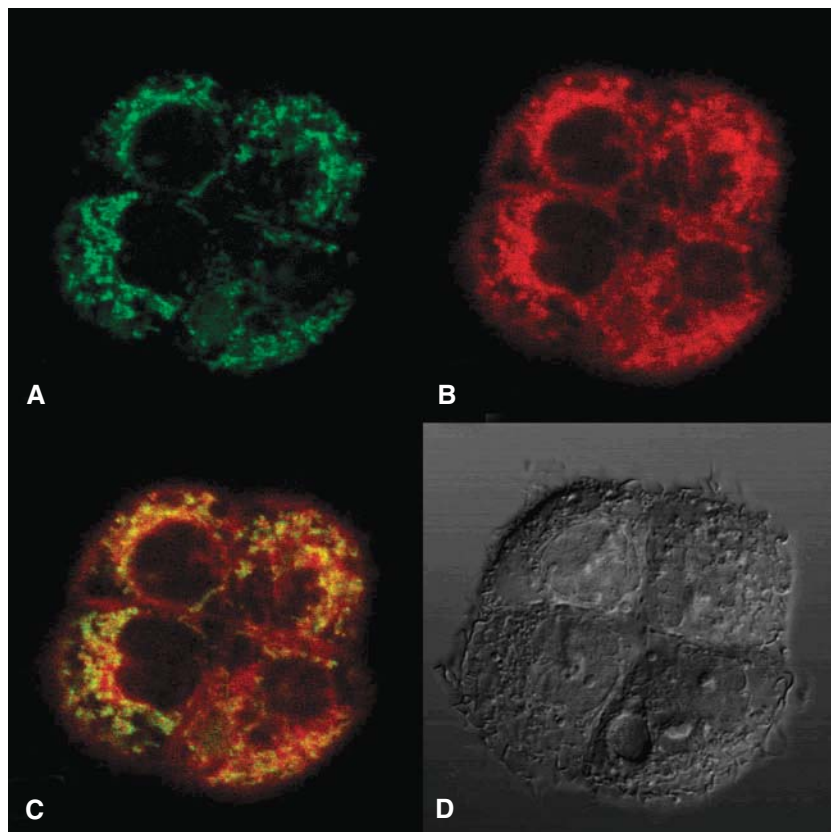


**Figure 40-7** The predominantly mitochondrial localization of the photosensitizer BPD-MA by confocal laser scanning microscopy. OVCAR-3 cells were incubated in 92 mmol/L BPD-MA for 3 h and 10 mmol/L rhodamine 123, a mitochondrial probe, for 20 min. **A**, Green fluorescence of rhodamine 123; **B**, red BPD-MA fluorescence; **C**, combination of A and B, where yellow indicates colocalization; **D**, Differential interference contrast transmission image. (Four-color version of figure on CD-ROM)

extremely rapid process and is shown in Figure 40-8.<sup>117</sup> The mechanisms behind this rapid induction have now partly been elucidated and, in general, are consistent with the hypothesis of Liu and colleagues,<sup>118</sup> which proposes the release of cytochrome *c* from mitochondria being a critical signal for the induction of apoptosis. Following PDT with a different photosensitizer, a very early step is the loss of cytochrome *c* into the cytosol.<sup>119–121</sup> In addition, a rapid loss of mitochondrial membrane potential is observed on PDT attributed to the opening of the so-called mitochondrial transition pore.<sup>122</sup> The loss of cytochrome *c* after PDT results in a sharp increase of caspase (cysteine protease acting on aspartic acid) 3 activity via complex formation with dATP (deoxyadenosine triphosphate),<sup>120</sup> apoptosis-activating factor-1 (APAF-1), and procaspase 9, and subsequent cleavage of procaspase 9 can activate procaspase 3.<sup>123,124</sup> Caspase 3 is a key player in the induction of apoptosis and involved in the cleavage of a number of proteins,<sup>125</sup> including deoxyribonucleic acid (DNA) fragmentation factor (DFF) and poly-ADP-ribose polymerase (PARP). The latter are involved in the final steps of the apoptotic process. Photodynamic treatment with the photosensitizers Pc4 (a silicon phthalocyanine, see Figure 40-1), BPD-MA, and aluminium phthalocyanine (AIPc) induces cleavage of PARP in different cell lines.<sup>117,126,127</sup> In addition, DFF activation occurs after PDT.<sup>119</sup> Figure 40-8 shows the very rapid

induction of PARP cleavage in LY-R cells after Pc4-mediated PDT, which is PDT dose dependent and can occur within 10 min following illumination.

Another aspect of PDT-induced apoptosis relevant to oncologic applications is that it appears to bypass the usual pathways for apoptotic control. Bcl-2, a protein found in the outer membrane of the mitochondria, is known to be an antiapoptotic moiety. The overexpression of this protein is associated with chemotherapy and radiation resistance.<sup>128</sup> Consistent with these observations, it was reported that in Chinese hamster ovary cells, the presence of Bcl-2 partly protects against apoptosis induction by photodynamic treatment with Pc4.<sup>129</sup> This could be a result of the known antioxidant effect of Bcl-2 or of its ability to

interfere with calcium homeostasis, which plays a role in photodynamically induced cell death.<sup>130</sup> However, it is more likely that Bcl-2 is involved in the inhibition of the cytochrome *c* release after PDT, known to be an important mechanism of modulation of apoptosis by Bcl-2.<sup>131,132</sup> Similarly, it was shown that PDT with BPD-MA was less effective in apoptosis induction in HL-60 cells overexpressing Bcl-2.<sup>133</sup> In these cells, the activation of caspases 3 and 6 was also diminished, indicating again their key role in PDT-induced apoptosis. In accordance with these results, it was shown that blocking of Bcl-2 by using retrovirus transfection with antisense Bcl-2 increases the sensitivity of MGC803 cells to PDT-induced apoptosis.<sup>134</sup> However, a reversal of the conventional inverse relationship between Bcl-2 expression and apoptosis induction was shown in an interesting study by Kim and colleagues.<sup>135</sup> Using AIPc as sensitizer, an enhanced sensitivity of a Bcl-2-transfected breast cancer cell line was demonstrated. This unexpected result was explained by the simultaneous increase in Bax, a proapoptotic Bcl-2 family member. It was postulated that Bcl-2 might be preferentially damaged by PDT, thereby increasing the Bax:Bcl-2 ratio, which subsequently leads to enhanced apoptosis. These observations are of significance in cancer therapy because, as mentioned above, overexpression of Bcl-2 is often involved in resistance mechanisms against chemotherapeutic agents.<sup>128</sup>

Studies<sup>136–138</sup> show the involvement of a different signal transduction cascade in growth arrest and apoptosis induced by PDT using Pc4. The WAF1/CIP1/p21 protein, which is an inhibitor of cyclin kinases was induced after PDT. This induction in turn, is believed to lead to the inhibition of cyclin D1 and D2 and their catalytic subunits cyclin-dependent kinase 2 (cdk2) and cdk6. These processes result in an arrest of the cells in the G0/G1 phase of the cell cycle. It was suggested that the increase in WAF1/CIP1/p21 and the subsequent induction of growth arrest was induced by nitric oxide (NO), produced during PDT.<sup>139</sup> In a follow-up study, it was shown that PDT, using Pc4, can cause hypophosphorylation of retinoblastoma protein (Rb), and inhibit free E2F.<sup>137</sup> E2F is a family of transcription factors, which regulate the G1-S transition in the cell cycle, and its inhi-

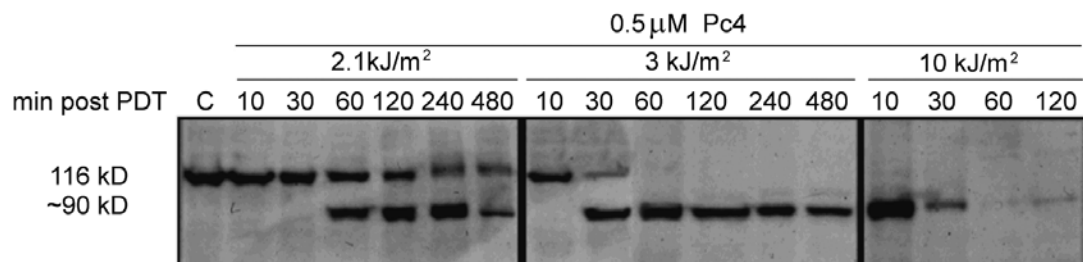


**Figure 40-8** Kinetics of poly-ADP-ribose polymerase (PARP) cleavage in LY-R cells induced by PDT with the photosensitizing agent Pc4 as a function of light dose. LY-R cells were exposed to 0.5 μM Pc4 and either 2.1, 3 or 10 kJ/m<sup>2</sup> of red light. At the indicated times thereafter, cells were collected, subjected to SDS-PAGE (sodium dodecyl sulfate–polyacrylamide gel electrophoresis), transferred and reacted with the 4C10-5 antibody. Reproduced with permission from He et al.<sup>117</sup>

bition causes arrest of the cells in the G0/G1 phase. This is the final step in the cascade involved in cell-cycle regulation that is affected by PDT. By using cells transfected with the viral protein E6, which abrogates *p53* function, Fisher and colleagues<sup>140</sup> showed that PDT with PF caused hypophosphorylation of Rb and subsequent cell-cycle arrest. Growth arrest was independent of the *p53* status of the cells, but the apoptotic response was clearly diminished in the cells without functional *p53*. However, despite the abrogation of the *p53*-mediated apoptotic pathway, the clonogenic survival following PDT was similar for cells with wild-type *p53* or cells with abrogated *p53* function. Cells resistant to apoptosis might, therefore, still be sensitive to PDT. Furthermore, a mutation in *p53*, which occurs in about 50% of human tumors, does not seem to influence its sensitivity to PDT.

Besides the apoptotic pathways described above, other signaling molecules have been implicated in the induction of apoptosis after PDT, such as ceramide formed after activation of sphingomyelinase by PDT.<sup>141,142</sup> In addition, phospholipases A and C have been shown to play a role in PDT-induced apoptosis.<sup>143</sup> The modulating effect of different kinases on the apoptosis induction by PDT is not well understood, but several recent studies have implicated the stress-activated kinases SAPK/JNK and p38/HOG1 in the control of apoptosis,<sup>144,145</sup> as well as the non-receptor-mediated tyrosine kinase Etk/bmx.<sup>146</sup> Apart from a necrotic or apoptotic response, cells can also undergo a rescue response after PDT, dependent on cell type, photosensitizer, and PDT dose. Several stress proteins involved in cell rescue have been shown to be upregulated following PDT: heat shock proteins,<sup>121,147,148</sup> glucose-regulated proteins,<sup>149–151</sup> and heme oxygenase.<sup>152</sup> In addition, phospholipase A, prostaglandin E<sub>2</sub>, and cyclic adenosine monophosphate (cAMP) were implicated in cellular rescue responses after PDT.<sup>130,153,154</sup>

PDT has also been shown to regulate adhesion molecules,<sup>155</sup> surface receptors such as major histocompatibility complex (MHC) classes I and II,<sup>156</sup> and a number of cytokines.<sup>157–159</sup> Cytokine induction by PDT has been shown to be under control of various transcription factors, such as AP-1 and NFκB.<sup>160</sup> These cellular changes probably play a role in the induction of an immune response after PDT, which is being exploited for developing new therapies.

**IN VIVO MECHANISMS** For most sensitizers in clinical and preclinical use, three primary mechanisms of PDT-mediated tumor destruction *in vivo* have been proposed: cellular, vascular, and immunologic. The relative contribution of each depends, among other factors, on the nature of the photosensitizer and its localization within the tumor tissue, tumor type (vascularity and macrophage content), and the time delay of irradiation after photosensitizer administration (which is one determinant of site of localization, eg, vascular vs parenchymal). The two most

investigated mechanisms *in vivo* are viewed as involving (1) direct tumor cell photoinactivation and (2) vascular destruction. The third, immunologic, is currently being investigated intensively in many laboratories, and a substantial understanding of this pathway can be anticipated in the near future.<sup>161–163</sup> The PDT response with any photosensitizer involves an interplay of all pathways. For example, using *in vivo*–*in vitro* analyses, Henderson and Dougherty<sup>18</sup> showed that the photosensitizer bacteriochlorophyll *a* has a direct cell-kill potential of ~50% at the end of the light treatment and exhibits no vascular shutdown until 3 to 4 h after the termination of irradiation. On the other hand, with PF, vascular shutdown begins almost immediately after the initiation of light exposure. Direct cell destruction is expected to dominate when the photosensitizer content is high within the tumor cells at the time of light activation. The actual mechanisms of cell death were discussed above in some detail, and the initial event may be simple organelle damage, such as membrane lipid peroxidation, disruption of lysosomal membrane, loss of mitochondrial membrane potential, and membrane enzyme inhibition.<sup>164</sup> Under the typical protocols, vascular damage is considered the dominant mechanism of tumor death *in vivo* for most photosensitizers being investigated clinically. Damage is believed to be initiated by release of factors such as eicosanoids, in particular thromboxane,<sup>165</sup> histamines, and tumor necrosis factor-α (TNF-α).<sup>159</sup> Macroscopically, the vascular PDT response is characterized by acute erythema, edema, blanching, and sometimes necrosis. Microscopically, the tumor tissue is characterized by endothelial cell damage,<sup>18,166</sup> platelet aggregation, vasoconstriction, and hemorrhage following PDT.<sup>90</sup> That a clean dissection of the mechanism(s) responsible for PDT-induced tumor destruction is not possible was pointed out in elegant studies.<sup>167,168</sup> RIF cells in which PDT resistance had been induced *in vitro* were implanted in mice and subjected to PF-mediated PDT under typical conditions in which a shutdown of the vasculature is generally believed to be the dominant mode of tumor destruction. As the resistance to PDT was induced within the tumor cells, it was expected that *in vivo* the tumor response to PDT (via vascular shutdown-induced hypoxia) would be similar for the parent and the resistant cell lines.<sup>168</sup> However, the observation was that the resistance to PDT was maintained *in vivo*, suggesting that direct cytotoxicity was a major component in the tumor photodestruction. As is the case with other modalities, extrapolation of *in vitro* observations to *in vivo* mechanisms is not always possible. Quite contradictory observations have been made; for example, while PF-mediated PDT *in vivo* causes platelet aggregation, photosensitization *in vitro* leads to an inhibition of platelet aggregation.<sup>169</sup>

It has been shown in some tumor treatments that the modulation of immune effects may play a role in PDT-induced destruction of tumors.<sup>13,159,162,170–177</sup> Nseyo and colleagues<sup>170</sup>

have reported high concentrations of interleukin (IL)-1β, IL-2, and TNF-α in the urine of patients treated with PDT for bladder cancer. The reason for the release of these cytokines and the role they may play in PDT are not well understood. In a study aimed at understanding the mechanisms responsible for PDT-induced potentiation of antitumor immunity, Gollnick and colleagues<sup>157</sup> demonstrated in a balb/c mouse model that PDT delivered to normal and tumor tissue *in vivo* causes marked changes in the expression of cytokines IL-6 and IL-10, but not TNF-α. IL-6 messenger ribonucleic acid (mRNA) and protein were strongly enhanced in the PDT-treated EMT6 tumor. PDT also increased IL-6 mRNA in exposed spleen and skin. The investigators concluded that the general inflammatory response to PDT may be mediated, at least in part, by IL-6. In contrast, IL-10 mRNA in the tumor decreased following PDT, while it was induced in the normal skin of mice exposed to a PDT regime that strongly inhibits the contact hypersensitivity response. The coincidence of the kinetics of IL-10 induction with the known kinetics of contact hypersensitivity inhibition observed in these studies suggests that the enhanced IL-10 expression is instrumental in the observed suppression of cell-mediated responses seen following PDT.

In an interesting approach to exploiting immune effects, Steele and colleagues<sup>171</sup> demonstrated that the selective photodestruction of suppressor T cells using monoclonal antibody-HP conjugates resulted in limited increased tumor regression in treated mice, compared with control mice. This enhanced regression was attributed to immune system stimulation after irradiation, leading to the increased killing activity of specific cytotoxic T lymphocytes against target tumor cells. Enhanced NK-cell activity following PDT was also suggested to be operative by possibly lowering the metastatic potential of surviving tumor cells.<sup>172,173</sup> Increased immunity by colony inhibition assays was also demonstrated in mice treated with BPD-MA-mediated PDT.<sup>174</sup> Macrophage involvement (TNF-α production) has been reported and studied by Korbelik and colleagues.<sup>162,176,178</sup> Studies show that tumor-associated macrophages accumulate up to nine times the PF levels present in tumor cells. This enhanced accumulation is attributed to the association of most porphyrins with LDL.<sup>177</sup> In addition to the direct release from macrophages of factors such as TNF-α that may mediate phototoxicity, an indirect mechanism of macrophage-mediated cytotoxicity in PDT has also been suggested.<sup>179</sup> According to this hypothesis, initial PDT-induced damage to tumor cells forms exposed lipid fragments. These fragments are then recognized as targets by macrophages. This recognition of possibly reparable cells by macrophages and subsequent phagocytosis is then responsible for tumor cell cytotoxicity. The observation of immune response stimulation in tumor treated with PDT has initiated a new hypothesis that PDT-mediated vaccines could be produced more effectively than by other means, and work by Gollnick and col-

leagues has indicated that this may be true.<sup>163</sup> In addition to the above evidence of immune stimulation, immune suppression has also been reported following PDT with both PF and BPD-MA.<sup>180,181</sup> This observed immune system suppression is being investigated for novel applications, such as organ transplantation and the treatment of autoimmune diseases.

### PHOTODYNAMIC THERAPY DOSIMETRY

In principle, photodynamic response is obtained wherever a photosensitizer, oxygen, and light occur simultaneously. Early studies indicated that the presence of photosensitizer and light were of equal importance, and that there existed some level of drug–light reciprocity in the tissue response,<sup>182,183</sup> in that decreasing the drug level by some factor would cause the same loss of effect, equivalent to alternatively decreasing the light delivered by the same factor. This reciprocity is lost in the presence of additional mitigating factors such as photobleaching, oxygen limitation, and excessive photosensitizer concentration leading to self-shielding of the light delivered.<sup>184,185</sup> The extent of the tissue response is modulated by the amounts of both the photosensitizer and the light, and in general, it varies in a dose-dependent manner for both. There appears to be a threshold component for PDT effects to be lethal,<sup>186–190</sup> below which tissue damage is repairable. This threshold value can be different for tumor and normal tissue providing an opportunity for added selectivity,<sup>190</sup> as well as varying between photosensitizers and with time after injection.<sup>189</sup>

However, the drug–light dependence of some photosensitizers is especially complex, such as with ALA-PpIX where the photosensitizer is produced within the cells after injection of ALA. The maximal production of PpIX is observed at 4 to 6 h after injection, and there is a complex interaction between optical dose rate and the magnitude of the effect observed. Recent observations have shown that a pretreatment of light followed by a dark interval of 2 h to allow regeneration of PpIX significantly increases the PDT effect, as measured in normal mouse skin, and variations of this dosimetric regimen will likely become important to maximize the efficacy of the treatment.<sup>191–193</sup> Dose rate effects are thought to be inherently linked to oxygen dependency, as is discussed further below.

**IN VIVO LIGHT DOSIMETRY** While the significance of accurate light delivery in PDT has been known for decades,<sup>22–24,194–196</sup> many clinical PDT studies have ended without success because of problems with delivering the appropriate amount of light to the tissue,<sup>197</sup> or from over delivery of light causing perforations or strictures.<sup>197,198</sup> Intracavity irradiation requires the use of specialized delivery probes and monitoring systems,<sup>22,199,200</sup> which allow delivery of light equally to the walls of the tissue, and incorporate integrating sphere effects into the dose calcula-

tions. In larger bulk tissues, prediction of the light fluence within the tissue is complicated because it requires accurate estimation of the tissue absorption, scatter and anisotropy parameters along with analytic or computational means to predict the light fluence. Elaborate methods to measure the interaction parameters have been developed,<sup>201–204</sup> and relatively simple expressions for diffusion theory prediction of light propagation in tissue-like media have been derived.<sup>186,195</sup> Probes that can be placed on the surface of tissue have been developed by several investigators and companies, and perhaps offer the easiest and most reliable method to estimate light dose to the surface of a tissue.<sup>22,205–207</sup> Integrated systems that measure the fluence rate either interstitially or on the surface of the tissues being treated are being implemented in many academic clinical PDT centers, but have not been integrated into commercial PDT treatments as of yet.<sup>207–209</sup>

**IN VIVO PHOTSENSITIZER DOSIMETRY** Measurement of photosensitizer concentration in tissue has been an issue of significant interest for several decades, with the most accepted method of quantification being biopsy sampling of the tissue and chemical extraction of the compound to be quantified by spectrophotometric assay.<sup>210,211</sup> Throughout this time, there has been interest in using the fluorescent properties of the photosensitizer to directly measure the concentration in vivo,<sup>194</sup> and useful qualitative case studies have shown the data has been largely confounded by variations in tissue optical properties, drug localization and aggregation variations which can all alter the intensity of the fluorescence detected independently of the absolute concentration.<sup>212</sup> More recently some probes have been developed which allow quantitative measurement of the fluorescence from small fiber systems which are below the length scale of scattering within tissue, thereby limiting the effect of tissue optical properties.<sup>211,213,214</sup> Clinical implementation of some elegant fluorescence-based methods currently exists.<sup>215</sup>

Photobleaching of the drug during irradiation has largely been ignored, but has become especially important with the increased use of ALA-PpIX photosensitization because it appears to have a rapid photobleaching rate.<sup>68,188,191,192,216–218</sup> Wilson and colleagues suggest using photobleaching of the photosensitizer as an indirect measure of the deposited PDT dose in the tissue, because the integrated loss of signal is an indirect measure proportional to the singlet oxygen produced, assuming that singlet oxygen mechanisms are causing the photodegradation.<sup>208</sup> Alternatively, others suggest the photobleaching degradation products that are optically active could be used to monitor the deposited dose.<sup>219–221</sup> This work continues in search of a good method to quantify deposited dose in tissue.

**IN VIVO OXYGEN DOSIMETRY** With most photosensitizers under investigation, in addition to amounts of photosensitizer and light, PDT effi-

cacy is also oxygen dependent.<sup>222–229</sup> It is generally accepted that the oxygen dependence is based on the requirement to form the active species, singlet oxygen from interaction of the excited photosensitizer with molecular oxygen dissolved in the tissue. This concept was mostly based on extrapolation from solution chemistry because the detection of singlet oxygen in vivo was not possible until very recently.<sup>230–233</sup> Other reactive oxygen species, such as hydroxyl radicals and superoxide anion, could also be important active species with some photosensitizers, although this remains to be proven in vitro or in vivo.<sup>234</sup> Under anoxic conditions, the PDT effects of PF are abolished.<sup>235</sup> It should be noted that the relationship between tumor blood flow or oxygen concentration and PDT is not a simple one, as demonstrated in the study by Fingar and colleagues,<sup>236</sup> in which the artificial oxygen carrier Fluosol-DA (20%) did not enhance PDT tumor destruction. Similarly, Iinuma and colleagues<sup>68</sup> demonstrated that in contrast to results from ionizing radiation, pretreatment of animals with nicotinamide, a homogenizer of tumor blood flow and oxygen concentration, did not enhance PDT response. In contrast to these observations, increased respiratory oxygen tension of 100% does enhance PDT efficacy with PF.<sup>237</sup>

An interesting consequence of this oxygen dependence is the effect of the fluence rate (the rate of photon delivery) on PDT efficiency. Within the range of fluence rates for linear photochemistry, there should be no effect of fluence rate on the efficacy of PDT assuming that there is an overabundance of oxygen available. In a clinical situation, higher subthermal fluence rates have been thought to be favorable because total

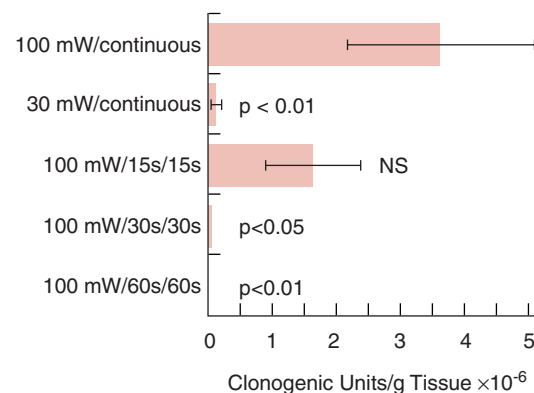


**Figure 40-9** The effect of fluence rate and light fractionation on BPD-mediated PDT. BPD-MA was administered to rats with NBT II tumors implanted into the bladder wall. One hour later, tumors were exposed to a total fluence of 30 J/cm<sup>2</sup> of 690-nm irradiation under the following conditions: 100 mW/cm<sup>2</sup> continuous; 100 mW/cm<sup>2</sup> fractionated 15 s on/15 s off; 100 mW/cm<sup>2</sup> 30 s on/30 s off; 100 mW/cm<sup>2</sup> 60 s on/60 s off. Tumors were disaggregated 24 h later and tumor cells were plated for colony formation assay. Colonies (50 cells or more) were counted 9 days later after fixing with methanol and staining with crystal violet. The Wilcoxon rank sum test was used to compare the number of clonogenic cells with data at 100 mW/cm<sup>2</sup> and continuous wave irradiations. Reproduced with permission from Iinuma et al.<sup>68</sup> NS = not significant.

irradiation time can be shortened. However, as shown in Figure 40-9, reduced efficacy of tumor destruction<sup>68,225,226,229</sup> has been reported when fluence rates, in the range typically applied in clinical studies (~100 to 200 mW/cm<sup>2</sup>), were used in PDT. This lowered effect has been attributed to oxygen depletion during the irradiation caused by oxygen consumption in the photochemical reaction at a rate greater than the rate of reperfusion. In vitro measurements and photochemical calculations confirm that an oxygen limitation to singlet oxygen production should exist in vivo when the available oxygen supply is limited and when the optical fluence rate and photosensitizer concentration in tissue are both high.<sup>227,238–243</sup>

Depletion of oxygen during photoirradiation has been investigated either by measuring the hypoxic cell fraction in the tumor immediately after PDT<sup>224</sup> or by directly measuring tissue oxygen tension during irradiation, using oxygen electrodes of various types.<sup>228,244–246</sup> The exact changes during PDT remain complex to discern exactly because of the problems of sampling small spatial regions with electrodes, and because the response is highly heterogeneous. Observations have shown both increases and decreases in oxygen tension following PDT,<sup>247,248</sup> indicating high degrees of heterogeneity occur and the response depends significantly upon the photosensitizer and protocol used.<sup>249</sup> Oxygen reduction during PDT has important practical implications and may be an important limitation of PDT. Tumor tissues are not homogeneous and may contain fractions of hypoxic cells, as the induction of neovessels lags tumor growth. In the extreme case, tumor necrosis occurs from lack of nutrients as well as lack of oxygen. It occurs especially in such hypoxic regions that PDT may be less effective because of the limited availability of oxygen.<sup>224,226</sup> Even for the tumor cells located near blood vessels, oxygen might become depleted when high fluence rates are used, consuming oxygen faster than it is replaced from the circulating blood. This problem can be obviated to some extent by using lower fluence rates or fractionated irradiation, as shown in preclinical studies.<sup>73,229,250–254</sup> In studies in an orthotopic rat bladder tumor model, Iinuma and colleagues<sup>68</sup> showed that at the fluence rate of 100 mW/cm<sup>2</sup> and total cumulative light dose of 30 J/cm<sup>2</sup>, PDT mediated by BPD-MA was enhanced almost 1,000-fold when a light fractionation regimen ( $\lambda = 690$  nm) of 60 s on and 60 s off was used (see Figure 40-9). At shorter intervals, the enhancement was absent or modest, presumably because oxygen depleted during the initial phase of PDT could not be replenished rapidly enough. Also, for the same fluence (30 J/cm<sup>2</sup>), tumor cell cytotoxicity was much enhanced when the fluence rate was 30 mW/cm<sup>2</sup> rather than 100 mW/cm<sup>2</sup>. Sitnik and colleagues<sup>228,246</sup> studied the effects of fluence rate on oxygen concentration in a murine RIF (radiation-induced fibrosarcoma) tumor model during and after PDT, using 5 mg/kg of PF and fluence rates of 30, 75, or 150 mW/cm<sup>2</sup>. Median PO<sub>2</sub> before

PDT ranged from 2.9 to 5.2 mm Hg in the three treatment groups. Within the first minute of illumination, median tumor pO<sub>2</sub> decreased with all fluence rates to values between 0.7 and 1.1 mm Hg. During prolonged illumination (20 to 50 J/cm<sup>2</sup>), PO<sub>2</sub> recovered at 30 mW/cm<sup>2</sup> fluence rate, but remained low at the 150 mW/cm<sup>2</sup> fluence rate (median PO<sub>2</sub> of 1.7 mm Hg). There was also a direct correlation between tumor regrowth times and recovery of oxygen levels within the tumor tissues. These preclinical studies appear to suggest that fluence rates lower than those being used currently should produce more efficient clinical PDT response. The problem that has to be addressed, then, is the practicality of treatment times and intervals. Fractionation needs to be accomplished within seconds to minutes and, in contrast to ionizing radiation, is ineffective at longer intervals of hours, possibly because of efficient repair mechanisms following PDT. The key exception to this rule is ALA-PpIX photodynamic therapy in which fractionation on the time scale of hours has shown a significant advantage, likely as a consequence of allowing increased production of PpIX in the intervening time period, although the exact mechanism of this enhancement is still to be determined.<sup>193</sup>

Recent studies show that following PDT with both PF and BPD-MA, tumor oxygenation can rise significantly above pretreatment values.<sup>247,249</sup> This rise can lead to increased radiation sensitivity as demonstrated by Pogue and colleagues,<sup>255</sup> and could lead to a new application for PDT as a useful adjuvant to radiation therapy of hypoxic tumors.

### PHOTODYNAMIC THERAPY WITH TARGETED MOLECULAR DELIVERY SYSTEMS

An important determinant of successful PDT targeting is the localization of the photosensitizer in neoplastic tissue. Although most photosensitizers in their currently used formulations provide adequate selectivity for the limited indications that PDT is used for at this time, the reach and the ease of use would be greatly enhanced if significantly high selectivity accumulation in tumor tissues could be achieved. The threshold effect discussed above combined with the increased selective localization could minimize the need for precise light dosimetry and concerns of toxicity in complex sites, such as the abdominal cavity. To optimize photodynamic action, the idea of drug targeting as introduced by Ehrlich,<sup>256</sup> has also been applied to PDT. The basic assumption is that molecular delivery systems have an ability to interact selectively with their targets. The rationale for the use of molecular delivery systems for photosensitizers is similar to that for the delivery of chemotherapeutics and toxins. There are, however, two fundamental differences in the requirement in the photon- and the non-photon-based approaches. First, in conventional therapy, the drug has to be freed to elicit the appropriate biologic response. This is not a prerequisite when macromolecular carrier molecules are used for delivery of photosensitizers

in PDT.<sup>14,42,257</sup> Second, in PDT, the requirements for specificity of the delivery molecule are less stringent. This is a consequence of the inherent double selectivity mentioned earlier. As long as the delivery agent has preferential (not necessarily exclusive) affinity for the target tissue, improved selective photodestruction is expected. Therefore, motivations for carrier-mediated PDT are (1) increased concentrations of the photosensitizers at target sites; (2) the possibility of using non-tumor-localizing photosensitizers with efficient photochemistry, thus providing a greater repertoire of usable chemicals; and (3) broadening the application of PDT and minimizing the need for precise light dosimetry. The problems associated with the use of large molecules, such as complicated syntheses, transport barriers, and potential systemic toxicity, are similar for photoconjugates and for other conjugates. Although a variety of macromolecular carriers have been used to deliver photosensitizers,<sup>14,42,257</sup> only two examples, the first using monoclonal antibodies (MAbs) (photoimmunotargeting) and the second using LDLs, are discussed here.

**PHOTOIMMUNOTARGETING** Tumor targeting with antibodies is based on (1) the assumption that new antigens are present on tumor cells, and (2) the ability to obtain specific MAbs that recognize these antigens. Neoplastic transformation is assumed to generate new and specific antigenic components not present in normal tissue. In practice, this is not always true, and MAbs with uniquely high level of specificity for tumor markers are generally nonexistent. Many molecules considered tumor antigens probably represent quantitative differences in glycosylation patterns rather than distinct proteins. Photoimmunoconjugates differ from other immunoconjugates in that in the case of MAb-photosensitizer conjugates, no effector function for the MAb or antibody internalization is required for toxicity because active cytotoxic species can act effectively at the cell membrane level. However, internalized conjugates could be more effective. In cases where drug resistance (eg, via the enhanced P-glycoprotein pump efflux) may be a problem, MAb-photosensitizer conjugates may be expected to be unaffected as long as binding to the cell surface is not seriously impaired. The potential for cytotoxicity of antigen-negative cells due to the diffusivity of free radicals may also be considered an advantage, since tumors generally contain heterogeneous cell populations.

PDT with immunoconjugates has been reviewed.<sup>14,257</sup> In contrast to MAb-toxin or MAb-radionuclide conjugates, photoimmunotargeting requires conjugates with high photosensitizer-to-MAb ratios, which makes the syntheses complicated. The goal of any such synthesis should be to retain features essential for both photosensitizer and antibody activities and at the same time allow maximal photosensitizer incorporation. Two basic approaches for the synthesis of antibody-photosensitizer conjugates have been used: (1) photosensitizers are linked chemically to

MABs directly, and (2) photosensitizers are linked to MABs via polymers. The development of the latter two-step procedures was motivated by the need for high photosensitizer-to-MAB ratios without serious impairment of the binding capabilities of the MAB. The photosensitizer is bound to polymeric carriers in the first step, and the carriers are attached to the MAB in the second step. This method allows for a high photosensitizer-to-MAB ratio with only a small number of attachment sites on the MAB itself and, therefore, in principle, minimal losses in the immunoreactivity of the MAB. A variety of photosensitizer-carrying polymers have been used. These include dextrans,<sup>15,42</sup> polyglutamic acid (PGA),<sup>258–260</sup> polyvinyl alcohols (PVAs),<sup>261,262</sup> poly[*N*-(2-hydroxypropyl) methacrylamide],<sup>263,264</sup> and poly-L-lysines.<sup>265,266</sup> Because the antigen-binding capabilities of antibodies largely reside in the Fab portion of the antibodies, conjugation at sites removed from these antigen-recognition sites is most desirable, and such site-specific syntheses have recently been developed.<sup>42,258,259,267,268</sup>

In the first study of MAB–photosensitizer conjugates,<sup>269</sup> the photosensitizer HP was coupled directly to an MAB directed against the DBA/2J myosarcoma M-1. Modestly increased photosensitized inhibition of tumor growth in DBA/2J mice treated with these conjugates and light was demonstrated, compared with controls treated with HP, MAB, or light alone. In a more recent report, Vrouenraets and colleagues,<sup>270</sup> using a noninternalizable MAB targeted to head and neck squamous cell carcinoma and coupled directly to meta-tetra(hydroxyphenyl)chlorin (mTHPC), established increased tumor selectivity of the conjugates in vivo compared with the free photosensitizers. No in vivo therapeutic results were reported.

A different use of the Mew and colleagues<sup>269</sup> conjugate prepared by the direct coupling of an anti-T-cell MAB and HP was exemplified in a study by Steele and colleagues,<sup>271</sup> in which immune stimulation was demonstrated by targeting T-suppressor cells by using an MAB (B16G)–HP conjugate directed against an epitope on T-suppressor cells in DBA/2J mice. Photosensitized tumor regression, reported in 10% to 40% of the mice, was correlated with an increase in the killing activity of specific cytotoxic T lymphocytes against target tumor cells. Such an exploitation of immune stimulation may be a valuable application of photoimmunotargeting because it circumvents the problems of target accessibility encountered in solid tumors.

Since the original report by Mew and colleagues, a number of studies have reported on the selective destruction of target cells using photoimmunoconjugates, where large numbers of photosensitizers were linked to MABs via polymers. T-cell leukemia cells were selectively targeted with a conjugate synthesized from an anti-Leu-1 MAB linked to a chlorin e6 (Ce6) derivative, Ce6-monoethylene diamine monoamide (CMA) via a dextran.<sup>42</sup> Photochemical destruction of these same leukemia

cells and bladder carcinoma cells using appropriate MABs bound to CMA via PGA intermediaries instead of dextran has also been reported.<sup>258–260</sup> A different synthetic scheme used PVA as the carrier and BPD-MA as the photosensitizer.<sup>261,262</sup> Although this reaction scheme leads to a nonspecific linkage on the MAB, good affinity, specificity, and phototoxicity of the conjugate were reported, probably because of the minimal number of sites on the MAB involved in the linkage. All these investigations suffer from poor conjugate characterization and purification.

Elegant syntheses using PGA and dextran intermediaries have been developed that show clear, site-specific, covalent linkage of the photosensitizer CMA on the heavy chain of the antibody.<sup>260,267</sup> Light- and photosensitizer-dose-dependent killing of target melanoma cells<sup>267</sup> and ovarian cancer cells (from a cell line and from human ovarian cancer patients) (Figure 40-10)<sup>260</sup> and in a murine mouse model in vivo was shown.<sup>268,269</sup> A survival advantage in the same murine model was also demonstrated for animals treated with the same immunoconjugate and light dose (Figure 40-11) in all of the above investigations, and the specific site of photosensitizer attachment on the MAB was the carbohydrate moiety.

Clinical applications of photoimmunotherapy have lagged behind laboratory applications, probably because of the complexity of the approach: it involves the equivalent of the development of a new drug in terms of synthesis, purification, and characterization. Often the issue is complicated by the fact that the “new drug” being developed is a composite of two entities that have different proprietary base and agendas. In fact, there is a recent report where photoimmunoconjugates of MABs recognizing CA125 on human ovarian cancer cells were used in humans.<sup>272–275</sup> In this study, in addition to showing selective photocytotoxicity to target cells in vitro and in vivo in a tumor-bearing nude rat model, the investigators treated three patients with advanced ovarian cancer by intraperitoneal administration of 1 mg MAB-phthalocyanine conjugate in Ringer solution. At laparotomy (72 h after photoimmunoconjugate administration), after removal of gross tumor, the peritoneum was irradiated with 50 J/cm<sup>2</sup> 670-nm light, and histologic evidence of tumor cell death was obtained. Development of the application of PDT continues to broaden to sites such as the intraperitoneal cavity in efforts such as those led by the group at the University of Pennsylvania.<sup>207,276</sup>

In addition to MABs alone, a number of investigators have reported successful targeting in vitro by using liposome–MAB conjugates to obtain higher photosensitizer loading.<sup>187,188</sup> Because of the size and nature of antibody–liposome conjugates, the utility in vivo is likely to be highly limited. In some situations, such as the treatments of cancers affecting body cavities (eg, ovarian carcinoma), intravesical application in

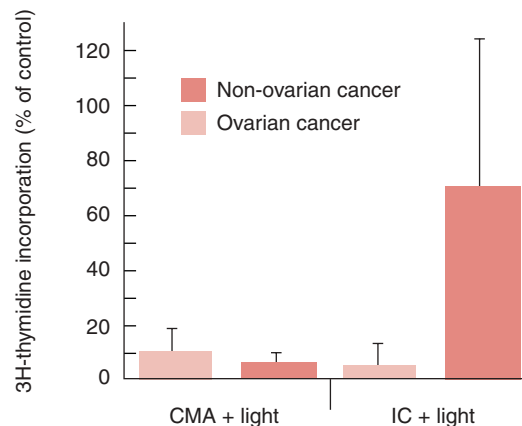


**Figure 40-10** Photoimmunotargeting of human ovarian cancer cells ex vivo. Cells from ascites of ovarian and nonovarian cancer patients were treated with immunoconjugate (IC) or the photosensitizer CMA alone for 1 h, washed with buffer, and irradiated with 25 J/cm<sup>2</sup> of 655 nm light. The IC used the MAB OC125, which recognizes the cell surface antigen CA125 on ovarian cancer cells. OC125 was conjugated to a chlorin derivative CMA via polyglutamic acid. Controls were IC and CMA without irradiation, irradiation alone, or no treatment. The error bars appear large because some of the nonovarian cancer cells showed high cell death. These cells were also high expressors of the relevant antigen CA125. Note that no difference is seen between ovarian and nonovarian cancer cells with CMA and irradiation. Reproduced with permission from Goff et al.<sup>260</sup>

bladder carcinomas, or extracorporeal treatments, these conjugates may be useful.

An interesting application of photoimmunotargeting was recently reported by Duska and colleagues.<sup>277</sup> Using ovarian cancer cells from human patients ex vivo, it was demonstrated that combination treatment of cisplatin (CDDP) and photoimmunotargeting using the MAB OC125 conjugated to a chlorin photosensitizer produced a 7-fold enhanced cytotoxicity over CDDP treatment alone. Interestingly, this enhancement was synergistic and greater for CDDP resistant cells (up to 13-fold). These and similar observations with other PDT agents<sup>190–193</sup> demonstrate the possibility of using PDT in the destruction of tumor cells that have developed resistance to chemotherapy agents.

In summary, the existing investigations of MAB–photosensitizer conjugates are promising. Better characterized and purified conjugates are needed, along with careful pharmacokinetic information in vivo in appropriate animal models. An aspect that is being explored is the use of photosensitizer–immunoconjugates synthesized with antibody fragments, synthetic MABs and fragments, and single-chain and chimeric antibodies. Such experiments will solve some of the problems associated with MAB transport and antispecies response. As a variety of photoimmunoconjugates becomes available, it will be important to establish the effect of the molecular features of the photoimmunoconjugates on their biologic behavior. Studies have shown that the molecular charge<sup>265,278</sup> may be critical in establishing the route of delivery for optimal selectivity. Similarly, the presence of enzyme-

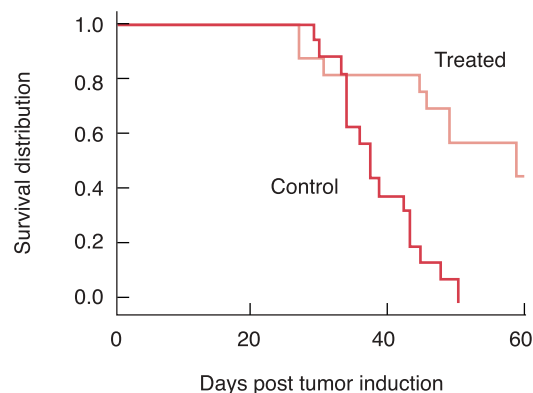


**Figure 40-11** Photoimmunotherapy of ovarian cancer in vivo. Ascites (NIH:OVCAR-3 cells)-bearing mice were treated with the same photoimmunoconjugate described in Figure 40-10. Twenty-four hours later, mice in the experimental group were treated with a total of 15 J of 656-nm irradiation intraperitoneally with a cylindrically diffusing fiber. The photoimmunotherapy was repeated three times, 1 week apart, and survival of the treated mice was compared with survival of untreated controls. Unpublished data from Goff and Hasan.

cleavable linkages could further enhance the efficacy of photoimmunoconjugates.

**TARGETING WITH LDLs** On the basis of the assumption that LDL plays an important role in tumor localization of photosensitizers, one strategy of photochemical targeting of tumor tissue has been to use LDL-complexed photosensitizers. One of the earlier studies along these lines, by Barel and colleagues<sup>93</sup> used HP precomplexed to LDL in murine MS-2 fibrosarcoma. An increased delivery of HP to the mouse tumor was reported with the HP-LDL complex, as compared with HP complexes of HDL, VLDL, or free HP. Similarly, precomplexing of BPD-MA with LDL led to a greater accumulation of the photosensitizers in tumors, as compared with administration of an aqueous BPD-MA solution at 3 h. This study,<sup>108</sup> which also compared BPD-MA delivery with complexes of VLDL, HDL, and serum, showed that by 4 h, the amount of BPD-MA had decreased for all cases (LDL, VLDL, serum, and free BPD-MA), except for the HDL complex, where an increase was noted. By 24 h, all three lipoprotein complexes had cleared from the tumor. Because skin phototoxicity is a major problem with PF, ratios of tumor to skin (R) are considered important. The R values from this study, summarized in Table 40-4, were optimal at 3 h. Influenced by such observations, photosensitizers covalently linked to LDL have been used to achieve improved PDT response. In one study,<sup>279</sup> it was shown that receptor-positive fibroblasts and retinoblastoma cells showed four- to fivefold enhancement in their PDT response (and photosensitizer uptake), as compared with receptor-negative cells and with the photosensitizer, either free or complexed with LDL.

An alternative way of delivering photosensitizers via the lipoprotein pathway involves the

use of liposomes. The concept, although not entirely clear, is that the liposome transfers its photosensitizer content efficiently to the lipoproteins, which then act as the true delivery agents.<sup>280</sup> Thus, in a comparison of the administration of aqueous HP and liposomal HP, it was demonstrated<sup>280</sup> that at 24 h and at 72 h, the photosensitizer content was higher for the liposomal delivery than for the aqueous delivery. The tumor to surrounding muscle ratio was also greater for the liposomal preparation. Table 40-5 summarizes the photosensitizer content in tumor and surrounding muscle in tissue from this study. Ratios were similar to those reported for BPD-MA above. Except for PF, most photosensitizers in experimental clinical use are packaged in liposomes or lipid emulsions. The reason for this is probably more the lack of solubility of these compounds in aqueous medium than the desire to deliver them via the LDL pathway.

An expected consequence of photosensitizer delivery with various macromolecular systems is the potentially differing mechanisms of tumor destruction as photosensitizers are delivered to different sites. For example, although albumin and globulins are believed to deliver photosensitizers mainly to the vascular stroma of tumors,<sup>280,281</sup> HDLs apparently deliver photosensitizers to cells via a nonspecific exchange with the plasma membrane. LDLs, as stated earlier, probably deliver a large fraction of the photosensitizer via an active receptor-mediated pathway.<sup>282-284</sup> Zhou and colleagues<sup>282</sup> suggest that aqueous solutions of HP lead to predominantly vascular damage, whereas LDL-mediated PDT leads predominantly to damage of neoplastic cells. An ultrastructure study of PDT with liposome-encapsulated ZnPc also claimed predominant tumor cell damage with a delayed and much-reduced vascular damage.<sup>285</sup> However, this is not always true. A recent study of PDT of ocular melanoma in a rabbit model used LDL complexed to BPD-MA. Despite the use of LDL as a carrier, early damage to the vasculature was demonstrated by light and electron microscopy.<sup>166</sup> The time that tumors are irradiated following administration of the photosensitizer is probably an important determinant of the

**Table 40-4 Tumor: Skin Ratios, (R) for BPD-MA Delivered in an Aqueous Formulation and Complexed to Lipoproteins<sup>a</sup>**

Formulation	Time		
	3h	8h	24h
BPD-MA (aq)	2.3	4.5	2.8
BPD-MA-LDL	5	2	1.4
BPD-MA-HDL	4	5	1.8
BPD-MA-VLDL	2.5	2.5	3.5

aq = Aqueous.  
<sup>a</sup>BPD-MA (4 mg/kg) was injected intravenously into tumor-bearing mice and was quantitated by extraction at various time points.  
 Data from Allison et al.<sup>107</sup>

**Table 40-5 Aqueous and Liposomal Hematoporphyrin Uptake by Tumor and Surrounding Muscle<sup>a</sup>**

Tissue	HP(aq)		HP(lip)	
	24 h	72 h	24 h	72 h
Tumor	1.0	0.6	2.5	2.0
Muscle	0.4	0.3	0.4	0.3
Ratio	2.5	2.0	6.3	6.7

aq = Aqueous; lip = liposomal.  
<sup>a</sup>HP (5 mg/kg) was administered to MS-2 fibrosarcoma bearing mice either in aqueous solution or incorporated into phosphatidylcholine liposomes. Data in  $\mu\text{g/g}$  of tissue.  
 Data from Jori.<sup>280</sup>

site of damage. Recent studies by Momma and colleagues<sup>286</sup> in an orthotopic rat bladder tumor model have shown that localization outside the vasculature of BPD occurs within hours, shifting the primary site of fluorescence away from the vasculature initially to the tissue parenchyma a few hours after injection. Similar localization patterns are observed in the RIF-1 tumor, as shown by Chen and colleagues,<sup>287</sup> where the change in localization also corresponds to a significant reduction in the damage occurring in the vasculature. Further study of the potential for photodynamic therapy towards different compartments of the tumor is likely to provide better disease-specific targeting applications.

## PERSPECTIVES

PDT has been an experimental clinical modality for the past two decades and has typically been used for palliative purposes in advanced cancers when other options failed. Because a large proportion of the patient population treated with PDT has been one whose cancers are refractory to all other treatments, the full potential of PDT has not yet been clearly evaluated in terms of cure rates. The clinical experience with several thousands of patients who have been treated with PDT is not discussed in any detail here; the clinical status has been reviewed rather comprehensively.<sup>12,13,19,288</sup> In general, all tumors appear to respond to the treatment; however, cure rates are not easily evaluated for a large proportion of the patient population. Limitations of light penetration make this therapy most appropriate for small and/or superficial lesions, such as bladder carcinoma in situ, early stage field cancerization of the oral mucosa, vulvar and early cervical cancers, early lung cancer, Barrett's esophagus, and cancers of the biliary tract. PDT may also have an important role in the purging of tumor cells from bone marrow or peripheral blood. In certain cases where relatively large solid tumors are in locations with delicate surrounding structures, PDT may be used with light administered interstitially using multiple fibers. Examples of such applications are tumors of the brain, prostate, and, in specific situations, residual disease in intraperitoneal carcinomatosis, as in ovarian and certain gas-

traintestinal malignancies. Increasing regulatory approval of this modality for some of the above indications has been encouraging and has stimulated research on new photosensitizers, better methods of localization, and improved resources for light delivery and dosimetry.

Table 40-1 lists initial regulatory approvals for PDT for a single photosensitizing agent. Since the last writing of this chapter, the field has moved rapidly and additional approvals have been obtained worldwide. PF has been granted orphan drug status for the treatment of high-grade dysplasia, associated with Barrett's esophagus, and has been submitted for approval for this indication in both the EU and the United States. Foscan (mTHPC) is approved in the EU for the palliative treatment of patients with head and neck squamous cell carcinoma failing prior therapies and unsuitable for radiotherapy, surgery or systemic chemotherapy. Levulan (5-ALA), a topical formulation, has been approved in the United States for the treatment of actinic keratosis. Metvix (5-ALA-methylester) is approved for the treatment of actinic keratosis and basal cell carcinoma in 14 European countries (including Germany and the United Kingdom) and in New Zealand. Market authorizations are pending in the United States, Australia, and Switzerland.

Overall, PDT has the potential of being a palliative therapy, a component of combination regimens (eg, with radio-, chemo-, and/or differentiation therapy), or a primary therapy depending on the specific indications. The photosensitizing agents used in PDT all have reasonable fluorescence, and this has spurred much activity in using these molecules for diagnostic purposes and for providing guidance for margins of resection. This aspect of photomedicine is at its infancy and may be expected to grow significantly in the near future with the development of newer technologies. Another interesting aspect of PDT that may be of importance in oncology, and in medicine in general, is that PDT is a dynamic process. As photosensitizers travel through different compartments of the tissue, the predominant site of damage (eg, cellular or vascular) could, to some extent, be selected by the choice of the timing of light exposure following photosensitizer administration. This could broaden the scope of application of this modality.

The long-term utility of PDT will be determined from results of well-designed controlled clinical trials, using selectively localized photosensitizers and convenient light sources, such as diode lasers, possibly with built-in light dosimetry components.

#### ACKNOWLEDGMENTS

Support of the authors was provided by National Institutes of Health Grants R01 AR40352 (T.H., A.M.), R01 CA78734 (B.W.P.), PO1 CA84203 (T.H., B.O., B.W.P.) and Office of Naval Research Contract N00014-94-1-0927 (B.O.) during the preparation of this chapter.

#### REFERENCES

- Raab C. Über die Wirkung fluoreszierender Stoffe auf Infusoria. *Z Biol* 1900;39:524-6.
- von Tappeiner HA, Jensionek A. Therapeutische Versuche mit fluoreszierenden Stoffen. *Münch Med Wochenschr* 1903;47:2042-4.
- von Tappeiner HA, Jensionek A. Die sensibilisierende Wirkung fluoreszierender Substanzen: gesammelte Untersuchungen über die photodynamische Erscheinung. Leipzig, Germany: Vogel; 1907.
- Meyer-Betz F. Untersuchungen über die biologische (photodynamische) Wirkung des Hämatoporphyrins und anderer Derivate des Blut- und Gallenfarbstoffs. *Dtsch Arch Klin Med* 1913;112:476-503.
- Figge FJ, Weiland GS, Manganiello LOJ. Cancer detection and therapy: affinity of neoplastic, embryonic, and traumatized tissues for porphyrins and metalloporphyrins. *Proc Soc Exp Biol Med* 1948;68:640-52.
- Lipson RL, Blades EJ. The photodynamic properties of a particular hematoporphyrin derivative. *Arch Dermatol* 1960;82:508-16.
- Kessel D, Chou TH. Tumor-localizing components of the porphyrin preparation hematoporphyrin derivative. *Cancer Res* 1983;43:1994-9.
- Dougherty TJ, Potter WR, Weishaupt KR. The structure of the active component of hematoporphyrin derivative. In: Doiron DR, Gomer CJ, editors. *Porphyrin localization and treatment of tumors*. New York: Alan R. Liss; 1984. p. 301-14.
- Dougherty TJ, Kaufman JE, Goldfarb A, et al. Photoradiation therapy for the treatment of malignant tumors. *Cancer Res* 1978;38:2628-35.
- Dougherty TJ, Lawrence G, Kaufman JH. Photoradiation in the treatment of recurrent breast carcinoma. *J Natl Cancer Inst* 1979;62:231-7.
- Dougherty TJ. Photosensitization of malignant tumors [review]. *Semin Surg Oncol* 1986;2:24-37.
- Marcus SL. Photodynamic therapy of human cancer. *Proc IEEE* 1992;80:869-86.
- Dougherty TJ, Gomer CJ, Henderson BW, et al. Photodynamic therapy. *J Natl Cancer Inst* 1998;90:889-905.
- Hasan T. Photosensitizer delivery mediated by macromolecular carrier systems. In: Dougherty GJ, Henderson B, editors. *Photodynamic therapy: basic principles and clinical applications*. New York: Marcel Dekker; 1992. p. 187-200.
- Strong L, Yarmush DM, Yarmush ML. Antibody targeted photolysis: photophysical, biochemical, and pharmacokinetic properties of antibacterial conjugates. *Ann N Y Acad Sci* 1994;745:297-320.
- Wilson BC, Patterson MS, Flock ST, Moulton JD. The optical absorption and scattering properties of tissues in the visible and near-infrared wavelength range. In: Dall'Acqua DM, editor. *Light in biology and medicine*. Vol. 1. New York: Plenum; 1988. p. 45-52.
- Dougherty TJ. Photosensitizers: therapy and detection of malignant tumors. *Photochem Photobiol* 1987;45:879-89.
- Henderson BW, Dougherty TJ. How does photodynamic therapy work? *Photochem Photobiol* 1992;55:145-57.
- Dougherty TJ, Marcus SL. Photodynamic therapy. *Eur J Cancer* 1992;28A:1734-42.
- Wilson BC. Photodynamic therapy: light delivery and dosage for second-generation photosensitizers [review]. *Ciba Found Symp* 1989;146:60-73.
- Wilson BC. Optical properties of tissues. In: *Encyclopedia of human biology*. Vol. 5. New York: Academic Press; 1991. p. 587-97.
- Wilson BC, Muller PJ, Yanch JC. Instrumentation and light dosimetry for intra-operative photodynamic therapy (PDT) of malignant brain tumours. *Phys Med Biol* 1986;31:125-33.
- Grossweiner LI, Hill JH, Lobraico RV. Photodynamic therapy of head and neck squamous cell carcinoma: optical dosimetry and clinical trial. *Photochem Photobiol* 1987;46:911-7.
- Star WM, Marijnissen JPA, van Gemert MJC. Light dosimetry in optical phantoms and in tissues: I. Multiple flux and transport theory. *Phys Med Biol* 1988;33:437-54.
- Shea CR, Hefetz Y, Gillès R, et al. Mechanistic investigation of doxycycline photosensitization by picosecond-pulsed and continuous wave laser irradiation of cells in culture. *J Biol Chem* 1990;265:5977-82.
- Smith G, McGimpsey WG, Lynch MC, et al. An efficient oxygen-independent two-photon photosensitization mechanism. *Photochem Photobiol* 1994;59:135-9.
- Dougherty GJ, Henderson BW. *Photodynamic therapy: basic principles and clinical applications*. New York: Marcel Dekker; 1992.
- Gomer CJ. Preclinical examination of first and second generation photosensitizers used in photodynamic therapy [review]. *Photochem Photobiol* 1991;54:1093-107.
- Bonnett R. Photosensitizers of the porphyrin and phthalocyanine series for photodynamic therapy. *Chem Soc Rev* 1995;24:19-33.
- Bolye RW, Dolphin D. Structure and biodistribution relationships of photodynamic sensitizers. *Photochem Photobiol* 1996;64:469-85.
- Peng Q, Moan J. Correlation of distribution of sulphonated aluminium phthalocyanines with their photodynamic effect in tumour and skin of mice bearing CaD2 mammary carcinoma. *Br J Cancer* 1995;72:565-74.
- Alian W, Andersson-Engels S, Svanberg K, Svanberg S. Laser-induced fluorescence studies of meso-tetra(hydroxyphenyl) chlorin in malignant and normal tissues in rats. *Br J Cancer* 1994;70:880-5.
- Pogue BW, Redmond RW, Trivedi N, Hasan T. Photophysical properties of tin ethyl etiopurpurin I (SnE2) and tin octaethylbenzochlorin (SnOEB) in solution and bound to albumin. *Photochem Photobiol* 1998;68:809-15.
- Pogue BW, Ortel B, Redmond RW, et al. A photobiological and photophysical-based study of phototoxicity of two chlorins. *Cancer Res* 2001;61:717-24.
- Aveline B, Hasan T, Redmond RW. Photophysical and photosensitizing properties of benzoporphyrin derivative monoacid ring A (BPD-MA). *Photochem Photobiol* 1994;59:328-35.
- Aveline BM, Hasan T, Redmond RW. The effects of aggregation, protein binding and cellular incorporation on the photophysical properties of benzoporphyrin derivative monoacid ring A (BPD-MA). *J Photochem Photobiol BPhotochem Photobiol* 1995;30:161-9.
- Schmidt-Erfurth U, Hasan T, Gragoudas E, et al. Vascular targeting in photodynamic occlusion of subretinal vessels. *Ophthalmology* 1993;101:1953-61.
- Schmidt-Erfurth U, Miller JW, Sickenberg M, et al. Photodynamic therapy of subfoveal choroidal neovascularization: clinical and angiographic examples. *Graefes Arch Clin Exp Ophthalmol* 1998;236:365-74.
- Miller JW, Schmidt-Erfurth U, Sickenberg M, et al. Photodynamic therapy with verteporfin for choroidal neovascularization caused by age-related macular degeneration: results of a single treatment in a phase 1 and 2 study [comment; see comments]. *Arch Ophthalmol* 1999;117:1161-73.
- Schmidt-Erfurth U, Miller JW, Sickenberg M, et al. Photodynamic therapy with verteporfin for choroidal neovascularization caused by age-related macular degeneration: results of retreatments in a phase 1 and 2 study. *Arch Ophthalmology* 1999;117:1177-87.
- Bressler NM. Photodynamic therapy of subfoveal choroidal neovascularization in age-related macular degeneration with Verteporfin: two-year results of 2 randomized clinical trials—Tap report 2. *Arch Ophthalmology* 2001;119:198-207.
- Oseroff AR, Ohuoha D, Hasan T. Antibody-targeted photolysis: selective photodestruction of human T-cell leukemia cells using monoclonal antibody-chlorin e6 conjugates. *Proc Natl Acad Sci U S A* 1986;83:8744-8.
- Cincotta L, Foley JW, Cincotta AH. Novel red absorbing benzo[a]phenoxazinium and benzo[a]phenothiazinium photosensitizers: in vitro evaluation. *Photochem Photobiol* 1987;46:751-8.
- Cincotta L, Foley JW, MacEachern T, et al. Novel photodynamic effects of a benzophenothiazine on two different murine sarcomas. *Cancer Res* 1994;54:1249-58.
- Cincotta L, Szeto D, Lampros E, et al. Benzophenothiazine and benzoporphyrin derivative combination phototherapy effectively eradicates large murine sarcomas. *Photochem Photobiol* 1996;63:229-37.
- Hendrzak-Henion JA, Knisely TL, Cincotta L. Role of the immune system in mediating the antitumor effect of benzophenothiazine photodynamic therapy. *J Photochem Photobiol B* 1999;14:275-92.
- Kennedy JC, Pottier RH. Endogenous protoporphyrin IX, a clinically useful photosensitizer for photodynamic therapy. *J Photochem Photobiol BPhotochem Photobiol* 1992;14:275-92.
- Peng Q, Worloe T, Berg K, et al. 5-Aminolevulinic acid-based photodynamic therapy. Clinical research and future challenges. *Cancer* 1997;79:2282-308.
- Grant WE, Hopper C, MacRobert AJ, et al. Photodynamic

- therapy of oral cancer—photosensitization with systemic aminolevulinic acid. *Lancet* 1993;342:147–8.
50. Mustajoki P, Timonen K, Gorchein A, et al. Sustained high plasma 5-aminolevulinic acid concentration in a volunteer: no porphyric symptoms. *Eur J Clin Invest* 1992;22:407–11.
  51. Barr H, Shepherd NA, Dix A, et al. Eradication of high-grade dysplasia in columnar-lined (Barrett's) oesophagus by photodynamic therapy with endogenously generated protoporphyrin IX. *Lancet* 1996;348:584–5.
  52. Tan WC, Fulljames C, Stone N, et al. Photodynamic therapy using 5-aminolevulinic acid for oesophageal adenocarcinoma associated with Barrett's metaplasia. *J Photochem Photobiol B* 1999;53:75–80.
  53. Ell C, Gossner L. Photodynamic therapy. *Recent research. Cancer Res* 2000;155:175–81.
  54. Gossner L, Ell C. Photodynamic therapy of gastric cancer. *Gastrointest Endosc Clin N Am* 2000;10:461–80.
  55. Kriegmair M, Baumgartner R, Knüchel R, et al. Detection of early bladder cancer by 5-aminolevulinic acid induced porphyrin fluorescence. *J Urol* 1996;155:105–10.
  56. Koenig F, McGovern FJ, Larne R, et al. Diagnosis of bladder carcinoma using protoporphyrin IX fluorescence induced by 5-aminolevulinic acid. *BJU Int* 1999;83:129–35.
  57. Riedl CR, Daniltschenko D, Koenig, et al. Fluorescence endoscopy with 5-aminolevulinic acid reduces early recurrence rate in superficial bladder cancer. *J Urol* 2001;165:1121–3.
  58. Leunig A, Betz CS, Mehlmann M, et al. Detection of squamous cell carcinoma of the oral cavity by imaging 5-aminolevulinic acid-induced protoporphyrin IX fluorescence. *Laryngoscope* 2000;110:78–83.
  59. Betz CS, Stepp H, Janda P, et al. A comparative study of normal inspection, autofluorescence and 5-ALA-induced PpIX fluorescence for oral cancer diagnosis. *Int J Cancer* 2002;97:245–52.
  60. Baumgartner R, Huber RM, Schulz H et al. Inhalation of 5-aminolevulinic acid: a new technique for fluorescence detection of early stage lung cancer. *J Photochem Photobiol B* 1996;36:169–74.
  61. Mayinger B, Horner P, Jordan M, et al. Endoscopic fluorescence spectroscopy in the upper GI tract for the detection of GI cancer: initial experience. *Am J Gastroenterol* 2001;96:2616–21.
  62. Mayinger B, Neidhardt S, Reh H, et al. Fluorescence induced with 5-aminolevulinic acid for the endoscopic detection and follow-up of esophageal lesions. *Gastrointest Endosc* 2001;54:572–8.
  63. Hillemanns P, Weingandt H, Baumgartner R, et al. Photodetection of cervical intraepithelial neoplasia using 5-aminolevulinic acid-induced porphyrin fluorescence. *Cancer* 2000;88:2275–82.
  64. Duska LR, Wimberly J, Deutsch T, et al. Detection of female lower genital tract dysplasia using orally administered 5-aminolevulinic acid induced protoporphyrin IX: a preliminary study. *Gynecol Oncol* 2002;85:125–8.
  65. Kaneko S. [Intraoperative photodynamic diagnosis of human glioma using ALA induced protoporphyrin IX]. *No Shinkei Geka* 2001;29:1019–31.
  66. Stummer W, Stepp H, Moller G, et al. Technical principles for protoporphyrin-IX-fluorescence guided microsurgical resection of malignant glioma tissue. *Acta Neurochir (Wien)* 1998;140:995–1000.
  67. Stummer W, Stoher S, Novotny A, et al. In vitro and in vivo porphyrin accumulation by C6 glioma cells after exposure to 5-aminolevulinic acid. *J Photochem Photobiol B* 1998;45:160–9.
  68. Iinuma S, Schomacker KT, Wagnieres G, et al. In vivo fluorescence rate and fractionation effects on tumor response and photobleaching: photodynamic therapy with two photosensitizers in an orthotopic rat tumor model. *Cancer Res* 1999;59:6164–70.
  69. Berlin NI, Neuberger A, Scott JJ. The metabolism of  $\kappa$  aminolevulinic acid. *Biochemistry* 1956;64:80–100.
  70. Grant WE, Hopper C, MacRobert AJ, et al. Photodynamic therapy of oral cancer: photosensitisation with systemic aminolevulinic acid. *Lancet* 1993;342:147–8.
  71. Malik Z, Lugaci H. Destruction of erythroleukaemic cells by photoactivation of endogenous porphyrins. *Br J Cancer* 1987;56:589–95.
  72. Iinuma S, Farshi SS, Ortel B, Hasan T. A mechanistic study of cellular photodestruction with 5-aminolevulinic acid-induced porphyrin. *Br J Cancer* 1994;70:21–8.
  73. Hua Z, Gibson SL, Foster TH, Hilf R. Effectiveness of delta-aminolevulinic acid-induced protoporphyrin as a photosensitizer for photodynamic therapy in vivo. *Cancer Res* 1995;55:1723–31.
  74. Pourzand C, Reelfs O, Kvam E, Tyrrell RM. The iron regulatory protein can determine the effectiveness of 5-aminolevulinic acid in inducing protoporphyrin IX in human primary skin fibroblasts. *J Invest Dermatol* 1999;112:419–25.
  75. Rittenhouse-Diakun K, Van Leengoed H, Morgan J, et al. The role of transferrin receptor (CD71) in photodynamic therapy of activated and malignant lymphocytes using the heme precursor delta-aminolevulinic acid (ALA). *Photochem Photobiol* 1995;61:523–8.
  76. Gibson SL, Cupriks DJ, Havens JJ, et al. A regulatory role for porphobilinogen deaminase (PBGD) in delta-aminolevulinic acid (delta-ALA)-induced photosensitization? *Br J Cancer* 1998;77:235–43.
  77. Ortel B, et al. Differentiation enhances ALA-dependent photodynamic therapy in LNCaP prostate cancer cells. *Br J Cancer* 2002;87:1321–7.
  78. Ortel B, Chen N, Brissette J, et al. Differentiation-specific increase in ALA-induced protoporphyrin IX accumulation in primary mouse keratinocytes. *Br J Cancer* 1998;77:1744–51.
  79. Li G, Szweczk MR, Pottier RH, Kennedy JC. Effect of mammalian cell differentiation on response to exogenous 5-aminolevulinic acid. *Photochem Photobiol* 1999;69:231–5.
  80. Gaullier JM, Berg K, Peng Q, et al. Use of 5-aminolevulinic acid esters to improve photodynamic therapy on cells in culture. *Cancer Res* 1997;57:1481–6.
  81. Xiang W, Weingandt H, Liessmann F, et al. Photodynamic effects induced by aminolevulinic acid esters on human cervical carcinoma cells in culture. *Photochem Photobiol* 2001;74:617–23.
  82. Luksiene Z, Eggen I, Moan J, et al. Evaluation of protoporphyrin IX production, phototoxicity and cell death pathway induced by hexylester of 5-aminolevulinic acid in Reh and HPB-ALL cells. *Cancer Lett* 2001;169:33–9.
  83. Kloek J, Akkermans W, Beijersbergen van Henegouwen GM. Derivatives of 5-aminolevulinic acid for photodynamic therapy: enzymatic conversion into protoporphyrin. *Photochem Photobiol* 1998;67:150–4.
  84. Kloek J, Beijersbergen van Henegouwen GM. Prodrugs of 5-aminolevulinic acid for photodynamic therapy. *Photochem Photobiol* 1996;64:994–1000.
  85. Lange N, Jichlinski P, Zellweger M, et al. Photodetection of early human bladder cancer based on the fluorescence of 5-aminolevulinic acid hexylester-induced protoporphyrin IX: a pilot study. *Br J Cancer* 1999;80:185–93.
  86. Uehlinger P, Zellweger M, Wagnieres G, et al. 5-Aminolevulinic acid and its derivatives: physical chemical properties and protoporphyrin IX formation in cultured cells. *J Photochem Photobiol B* 2000;54:72–80.
  87. Roberts WG, Hasan T. Tumor-secreted vascular permeability factor/vascular endothelial growth factor influences photosensitizer uptake. *Cancer Res* 1993;53:153–7.
  88. Nelson JS, Liaw LH, Orenstein A, et al. Mechanism of tumor destruction following photodynamic therapy with hematoporphyrin derivative, chlorin, and phthalocyanine. *J Natl Cancer Inst* 1988;80:1599–605.
  89. Reed MW, Wieman TJ, Schuschke DA, et al. A comparison of the effects of photodynamic therapy on normal and tumor blood vessels in the rat microcirculation. *Radiat Res* 1989;119:542–52.
  90. Fingar VH, Taber SW, Haydon PS, et al. Vascular damage after photodynamic therapy of solid tumors: a view and comparison of effect in pre-clinical and clinical models at the University of Louisville. *In Vivo* 2000;14:93–100.
  91. Roberts WG, Hasan T. Role of neovasculature and vascular permeability on the tumor retention of photodynamic agents. *Cancer Res* 1992;52:924–30.
  92. Fingar VH, Kik PK, Haydon PS, et al. Analysis of acute vascular damage after photodynamic therapy using benzoporphyrin derivative (BPD). *Br J Cancer* 1999;79:1702–8.
  93. Barel A, Jori G, Perin A, et al. Role of high-, low- and very low-density lipoproteins in the transport and tumor-delivery of hematoporphyrin in vivo. *Cancer Lett* 1986;32:145–50.
  94. Bertoloni G, Zambotto F, Conventi L, et al. Role of specific cellular targets in the hematoporphyrin-sensitized photoinactivation of microbial cells. *Photochem Photobiol* 1987;46:695–8.
  95. Kessel D. Porphyrin-lipoprotein association as a factor in porphyrin localization. *Cancer Lett* 1986;33:183–8.
  96. Jori G. Low density lipoproteins-liposome delivery systems for tumor photosensitizers in vivo. In: Dougherty GJ, Henderson BW, editors. *Photodynamic therapy: basic principles and clinical applications*. New York: Marcel Dekker; 1992. p. 173–86.
  97. Kongshaug M, Moan J, Cheng LS, et al. Binding of drugs to human plasma proteins, exemplified by Sn(IV)-etiopurpurin dichloride delivered in cremophor and DMSO. *Int J Biochem* 1993;25:739–60.
  98. Kongshaug M, Moan J, Cheng LS, Morgan AR. Binding of etiopurpurin to human plasma proteins. Delivery in cremophor EL and dimethyl sulphoxide. III. *Int J Biochem Cell Biol* 1995;27:481–92.
  99. Kessel D, Thompson P, Saatio K, Nantwi KD. Tumor localization and photosensitization by sulfonated derivatives of tetraphenylporphine. *Photochem Photobiol* 1987;45:787–90.
  100. Winkelman JW. Quantitative studies of tetraphenylporphinesulfonate and hematoporphyrin derivative distribution in animal tumor systems. In: Kessel D, editor. *Methods in porphyrin sensitization*. New York: Plenum; 1985. p. 91–6.
  101. Evensen JF. In: Jori G, editor. *Photodynamic therapy of tumors and other diseases*. Padova, Italy: Libreria Progetto; 1985.
  102. Qian P, Evensen JF, Rimington C, Moan J. A comparison of different photosensitizing dyes with respect to uptake C3H-tumors and tissues of mice. *Cancer Lett* 1987;36:1–10.
  103. Kessel D. Determinants of photosensitization by mono-L-aspartyl chlorin e6 [published erratum appears in *Photochem Photobiol* 1989;50:1]. *Photochem Photobiol* 1989;49:447–52.
  104. Ferrario A, Kessel D, Gomer CJ. Metabolic properties and photosensitizing responsiveness of mono-L-aspartyl chlorin e6 in a mouse tumor model. *Cancer Res* 1992;52:2890–3.
  105. Roberts WG, Shiau FY, Nelson JS, et al. In vitro characterization of monoaspartyl chlorin e6 and diasparyl chlorin e6 for photodynamic therapy. *J Natl Cancer Inst* 1988;80:330–6.
  106. Gomer CJ, Ferrario A. Tissue distribution and photosensitizing properties of mono-L-aspartyl chlorin e6 in a mouse tumor model. *Cancer Res* 1990;50:3985–90.
  107. Allison BA, Pritchard PH, Richter AM, Levy JG. The plasma distribution of benzoporphyrin derivative and the effects of plasma lipoproteins on its biodistribution. *Photochem Photobiol* 1990;52:501–7.
  108. Allison BA, Pritchard PH, Levy JG. Evidence for low-density lipoprotein receptor-mediated uptake of benzoporphyrin derivative [published erratum appears in *Br J Cancer* 1995;71:214]. *Br J Cancer* 1994;69:833–9.
  109. Richter AM, Waterfield E, Jain AK, et al. Liposomal delivery of a photosensitizer, benzoporphyrin derivative monoacid ring A (BPD), to tumor tissue in a mouse tumor model. *Photochem Photobiol* 1993;57:1000–6.
  110. Richter AM, Jain AK, Obochi M, et al. Activation of benzoporphyrin derivative in the circulation of mice without skin photosensitivity. *Photochem Photobiol* 1994;59:350–5.
  111. Oleinick NL, Evans HH. The photobiology of photodynamic therapy: cellular targets and mechanisms. *Radiat Res* 1998;150:S146–56.
  112. Peng Q, Moan J, Nesland JM. Correlation of subcellular and intratumoral photosensitizer localization with ultrastructural features after photodynamic therapy. *Ultrastruct Pathol* 1996;20:109–29.
  113. Kessel D, Luo Y. Mitochondrial photodamage and PDT-induced apoptosis. *J Photochem Photobiol B* 1998;42:89–95.
  114. Kessel D, Luo Y, Deng Y, Chang CK. The role of subcellular localization in initiation of apoptosis by photodynamic therapy. *Photochem Photobiol* 1997;65:422–6.
  115. Dahle J, Steen HB, Moan J. The mode of cell death induced by photodynamic treatment depends on cell density. *Photochem Photobiol* 1999;70:363–7.
  116. Wood SR, Holroyd JA, Brown SB. The subcellular localization of Zn(II) phthalocyanines and their redistribution on exposure to light. *Photochem Photobiol* 1997;65:397–402.
  117. He J, Whitacre CM, Xue LY, et al. Protease activation and cleavage of poly(ADP-ribose) polymerase: an integral part of apoptosis in response to photodynamic treatment. *Cancer Res* 1998;58:940–6.
  118. Liu X, Kim CN, Yang J, et al. Induction of apoptotic program in cell-free extracts: requirement for dATP and cytochrome c. *Cell* 1996;86:147–57.
  119. Granville DJ, Carthy CM, Jiang H, et al. Rapid cytochrome c release, activation of caspases 3, 6, 7 and 8 followed by Bap31 cleavage in HeLa cells treated with photodynamic therapy. *FEBS Lett* 1998;437:5–10.
  120. Varnes ME, Chiu SM, Xue LY, Oleinick NL. Photody-

- dynamic therapy-induced apoptosis in lymphoma cells: translocation of cytochrome c causes inhibition of respiration as well as caspase activation. *Biochem Biophys Res Commun* 1999;255:673-9.
121. Kessel D, Luo Y. Photodynamic therapy: a mitochondrial inducer of apoptosis. *Cell Death Differ* 1999;6:28-35.
  122. Green DR, Reed JC. Mitochondria and apoptosis. *Science* 1998;281:1309-12.
  123. Thornberry NA, Lazebnik Y. Caspases: enemies within. *Science* 1998;281:1312-6.
  124. Nunez G, Benedict MA, Hu Y, Inohara N. Caspases: the proteases of the apoptotic pathway. *Oncogene* 1998;17:3237-45.
  125. Porter AG, Janicke RU. Emerging role of caspase-3 in apoptosis. *Cell Death Differ* 1999;6:99-104.
  126. Luo Y, Kessel D. Initiation of apoptosis versus necrosis by photodynamic therapy with chloroaluminum phthalocyanine. *Photochem Photobiol* 1997;66:479-83.
  127. Belzacq AS, Jacotot E, Vieira HL, et al. Apoptosis induction by the photosensitizer verteporfin: identification of mitochondrial adenine nucleotide translocator as a critical target. *Cancer Res* 2001;61:1260-4.
  128. van Brussel JP, Mickisch GH. Circumvention of multidrug resistance in genitourinary tumors. *Int J Urol* 1998;5:1-15.
  129. He J, Agarwal ML, Larkin HE, et al. The induction of partial resistance to photodynamic therapy by the protooncogene BCL-2. *Photochem Photobiol* 1996;64:845-52.
  130. Penning LC, Rasch MH, Larkin HE, et al. A role for the transient increase of cytoplasmic free calcium in cell rescue after photodynamic treatment. *Biochim Biophys Acta* 1992;1107:255-60.
  131. Yang J, Liu X, Bhalla K. Prevention of apoptosis by Bcl-2: release of cytochrome c from mitochondria blocked. *Science* 1997;275:1129-32.
  132. Kluck RM, Bossy-Wetzel E, Green DR, Newmeyer DD. The release of cytochrome c from mitochondria: a primary site for Bcl-2 regulation of apoptosis. *Science* 1997;275:1132-6.
  133. Granville DJ, Jiang H, An MT, et al. Bcl-2 overexpression blocks caspase activation and downstream apoptotic events instigated by photodynamic therapy. *Br J Cancer* 1999;79:95-100.
  134. Zhang WG, Ma LP, Wang SW, et al. Antisense bcl-2 retrovirus vector increases the sensitivity of a human gastric adenocarcinoma cell line to photodynamic therapy. *Photochem Photobiol* 1999;69:582-6.
  135. Kim HR, Luo Y, Li G, Kessel D. Enhanced apoptotic response to photodynamic therapy after bcl-2 transfection. *Cancer Res* 1999;59:3429-32.
  136. Whitacre CM, Feyes DK, Satoh T, et al. Photodynamic therapy with the phthalocyanine photosensitizer Pc 4 of SW480 human colon cancer xenografts in athymic mice. *Clin Cancer Res* 2000;6:2021-7.
  137. Ahmad N, Mukhtar H. Mechanism of photodynamic therapy-induced cell death. *Methods Enzymol* 2000;319:342-58.
  138. Colussi VC, Feyes DK, Mulvihill JW, et al. Phthalocyanine 4 (Pc 4) photodynamic therapy of human OVCAR-3 tumor xenografts. *Photochem Photobiol* 1999;69:236-41.
  139. Gupta S, Ahmad N, Mukhtar H. Involvement of nitric oxide during phthalocyanine (Pc4) photodynamic therapy-mediated apoptosis. *Cancer Res* 1998;58:1785-8.
  140. Fisher AM, Ferrario A, Rucker N, et al. Photodynamic therapy sensitivity is not altered in human tumor cells after abrogation of p53 function. *Cancer Res* 1999;59:331-5.
  141. Separovic D, He J, Oleinick NL. Ceramide generation in response to photodynamic treatment of L5178Y mouse lymphoma cells. *Cancer Res* 1997;57:1717-21.
  142. Separovic D, Mann KJ, Oleinick NL. Association of ceramide accumulation with photodynamic treatment-induced cell death. *Photochem Photobiol* 1998;68:101-9.
  143. Agarwal ML, Larkin HE, Zaidi SI, et al. Phospholipase activation triggers apoptosis in photosensitized mouse lymphoma cells. *Cancer Res* 1993;53:5897-902.
  144. Agostinis P, Assafa Z, Vantieghe A, et al. Apoptotic and anti-apoptotic signaling pathways induced by photodynamic therapy with hypericin. *Adv Enzyme Regul* 2000;40:157-82.
  145. Xue L, He J, Oleinick NL. Promotion of photodynamic therapy-induced apoptosis by stress kinases. *Cell Death Differ* 1999;6:855-64.
  146. Xue LY, Qiu Y, He J, et al. Etk/Bmx, a PH-domain containing tyrosine kinase, protects prostate cancer cells from apoptosis induced by photodynamic therapy or thapsigargin. *Oncogene* 1999;18:3391-8.
  147. Xue LY, He J, Oleinick NL. Rapid tyrosine phosphorylation of Hs1 in the response of mouse lymphoma L5178Y-R cells to photodynamic treatment sensitized by the phthalocyanine Pc 4. *Photochem Photobiol* 1997;66:105-13.
  148. Gomer CJ, Ryter SW, Ferrario A, et al. Photodynamic therapy-mediated oxidative stress can induce expression of heat shock proteins. *Cancer Res* 1996;56:2355-60.
  149. Gomer CJ, Ferrario A, Rucker N, et al. Glucose regulated protein induction and cellular resistance to oxidative stress mediated by porphyrin photosensitization. *Cancer Res* 1991;51:6574-9.
  150. Morgan J, Whitaker JE, Oseroff AR. GRP78 induction by calcium ionophore potentiates photodynamic therapy using the mitochondrial targeting dye victoria blue BO. *Photochem Photobiol* 1998;67:155-64.
  151. Xue LY, Agarwal ML, Varnes ME. Elevation of GRP-78 and loss of HSP-70 following photodynamic treatment of V79 cells: sensitization by nigericin. *Photochem Photobiol* 1995;62:135-43.
  152. Gomer CJ, Luna M, Ferrario A, Rucker N. Increased transcription and translation of heme oxygenase in Chinese hamster fibroblasts following photodynamic stress or Photofrin II incubation. *Photochem Photobiol* 1991;53:275-9.
  153. Penning LC, Vansteveninck J, Dubbelman T. Hpd-induced photodynamic changes in intracellular cyclic-AMP levels in human bladder transitional carcinoma-cells, clone-T24. *Biochem Biophys Res Commun* 1993;194:1084-9.
  154. Penning LC, Dubbelman TM. Fundamentals of photodynamic therapy - cellular and biochemical aspects. *Anti-cancer Drug* 1994;5:139-46.
  155. Runnels JM, Chen B, Ortel B, et al. BPD-MA-mediated photosensitization in vitro and in vivo: cellular adhesion and B1 integrin expression in ovarian cancer cells. *Br J Cancer* 1999;80:946-53.
  156. King DE, Jiang H, Simkin GO, et al. Photodynamic alteration of the surface receptor expression pattern of murine splenic dendritic cells. *Scand J Immunol* 1999;49:184-92.
  157. Gollnick SO, Liu X, Owczarczak B, et al. Altered expression of interleukin 6 and interleukin 10 as a result of photodynamic therapy in vivo. *Cancer Res* 1997;57:3904-9.
  158. Kick G, Messer G, Goetz A, et al. Photodynamic therapy induces expression of interleukin 6 by activation of AP-1 but not NF-kappa B DNA binding. *Cancer Res* 1995;55:2373-9.
  159. Evans S, Matthews W, Perry R, et al. Effect of photodynamic therapy on tumor necrosis factor production by murine macrophages. *J Natl Cancer Inst* 1990;82:34-9.
  160. Piret B, Legrand-Poels S, Sappey C, Piette J. NF-kappa B transcription factor and human immunodeficiency virus type 1 (HIV-1) activation by methylene blue photosensitization. *Eur J Biochem* 1995;228:447-55.
  161. Hunt DW, Chan AH. Influence of photodynamic therapy on immunological aspects of disease—an update. *Expert Opin Invest Drugs* 2000;9:807-17.
  162. Korbek M, Dougherty GJ. Photodynamic therapy-mediated immune response against subcutaneous mouse tumors. *Cancer Res* 1999;59:1941-6.
  163. Gollnick SO, Vaughan L, Henderson BW. Generation of effective antitumor vaccines using photodynamic therapy. *Cancer Res* 2002;62:1604-8.
  164. Dubbelman T. Porphyrin-photosensitized modification of subcellular structures. In: Jori G, editor. *Photodynamic therapy of tumors and other diseases*. Padova, Italy: Libreria Progetto; 1985. p. 93-5.
  165. Fingar VH, Wieman TJ, Doak KW. Role of thromboxane and prostacyclin release on photodynamic therapy-induced tumor destruction. *Cancer Res* 1990;50:2599-603.
  166. Schmidt-Erfurth U, Bauman W, Gragoudas E, et al. Photodynamic therapy of experimental choroidal melanoma using lipoprotein-delivered benzoporphyrin. *Ophthalmology* 1994;101:89-99.
  167. Fingar VH, Wieman TJ. Studies on the mechanism of photodynamic therapy induced tumor destruction. *Proc SPIE* 1990;1203:168-77.
  168. Adams K, Rainbow AJ, Wilson BC, Singh G. In vivo resistance to photofrin-mediated photodynamic therapy in radiation-induced fibrosarcoma cells resistant to in vitro Photofrin-mediated photodynamic therapy. *J Photochem Photobiol B* 1999;49:136-41.
  169. Henderson BW, Owczarczak B, Sweeney J, Gessner T. Effects of photodynamic treatment of platelets or endothelial cells in vitro on platelet aggregation. *Photochem Photobiol* 1992;56:513-21.
  170. Nseyo UO, Whalen RK, Duncan MR, et al. Urinary cytokines following photodynamic therapy for bladder cancer. A preliminary report. *Urology* 1990;36:167-71.
  171. Steele JK, Liu D, Stammers AT, et al. Suppressor deletion therapy: selective elimination of T suppressor cells in vivo using a hematoporphyrin conjugated monoclonal antibody permits animals to reject syngeneic tumor cells. *Cancer Immunol Immunother* 1988;26:125-31.
  172. Gomer CJ, Ferrario A, Murphree AL. The effect of localized porphyrin photodynamic therapy on the induction of tumour metastasis. *Br J Cancer* 1987;56:27-32.
  173. Gomer CJ, Ferrario A, Hayashi N, et al. Molecular, cellular, and tissue responses following photodynamic therapy [review]. *Lasers Surg Med* 1988;8:450-63.
  174. Logan PM, Newton J, Richter AM, Levy JG. Immunological effects of photodynamic therapy. *Proc SPIE* 1990;1203:153-8.
  175. Kros G, Korbek M. Potentiation of photodynamic therapy by immunotherapy: the effect of schizophyllan (SPG). *Cancer Lett* 1994;84:43-9.
  176. Korbek M, Sun J, Posakony JJ. Interaction between photodynamic therapy and BCG immunotherapy responsible for the reduced recurrence of treated mouse tumors. *Photochem Photobiol* 2001;73:403-9.
  177. Hamblin MR, Newman EL. On the mechanism of the tumor-localizing effect in photodynamic therapy. *J Photochem Photobiol B* 1994;23:3-8.
  178. Korbek M, Kros G. Photofrin accumulation in malignant and host cell populations of a murine fibrosarcoma. *Photochem Photobiol* 1995;62:162-8.
  179. Korbek M, Kros G. Enhanced macrophage cytotoxicity against tumor cells treated with photodynamic therapy. *Photochem Photobiol* 1994;60:497-502.
  180. Lynch DH, Haddad S, King VJ, et al. Systemic immunosuppression induced by photodynamic therapy (PDT) is adoptively transferred by macrophages. *Photochem Photobiol* 1989;49:453-8.
  181. Simkin GO, Obuchi MO, Hunt DW, Levy JG. Effect of photodynamic therapy using benzoporphyrin derivative on the cutaneous immune response. *Proc SPIE* 1995;2392:23-33.
  182. Bown SG, Tralau CJ, Smith PD, et al. Photodynamic therapy with porphyrin and phthalocyanine sensitisation: quantitative studies in normal rat liver. *Br J Cancer* 1986;54:43-52.
  183. Marijnissen JP, Versteeg JA, Star WM, van Putten WL. Tumor and normal tissue response to interstitial photodynamic therapy of the rat R-1 rhabdomyosarcoma. *Int J Radiat Oncol Biol Phys* 1992;22:963-72.
  184. Barr H, MacRobert AJ, Tralau CJ, et al. The significance of the nature of the photosensitizer for photodynamic therapy: quantitative and biological studies in the colon. *Br J Cancer* 1990;62:730-5.
  185. Moesta KT, Greco WR, Nurse-Finlay SO, et al. Lack of reciprocity in drug and light dose dependence of photodynamic therapy of pancreatic adenocarcinoma in vitro. *Cancer Res* 1995;55:3078-84.
  186. Patterson MS, Wilson BC, Graff R. In vivo tests of the concept of photodynamic threshold dose in normal rat liver photosensitized by aluminum chlorosulphonated phthalocyanine. *Photochem Photobiol* 1990;51:343-9.
  187. Farrell TJ, Wilson BC, Patterson MS, Chow R. The dependence of photodynamic threshold dose on treatment parameters in normal rat liver in vivo. *Proc SPIE* 1991;1426:146-155.
  188. Georgakoudi I, Nichols MG, Foster TH. The mechanism of Photofrin photobleaching and its consequences for photodynamic dosimetry. *Photochem Photobiol* 1997;65:135-44.
  189. Farrell TJ, Wilson BC, Patterson MS, Olivo MC. Comparison of the in vivo photodynamic threshold dose for photofrin, mono- and tetrasulfonated aluminum phthalocyanine using a rat liver model. *Photochem Photobiol* 1998;68:394-9.
  190. Lilje L, Wilson BC. Photodynamic therapy of intracranial tissues: a preclinical comparative study of four different photosensitizers. *J Clin Laser Med Surg* 1998;16:81-91.
  191. Robinson DJ, et al. Fluorescence photobleaching of ALA-induced protoporphyrin IX during photodynamic therapy of normal hairless mouse skin: the effect of light dose and irradiance and the resulting biological effect. *Photochem Photobiol* 1998;67:140-9.
  192. Robinson DJ, et al. Protoporphyrin IX fluorescence photobleaching during ALA-mediated photodynamic therapy of UVB-induced tumors in hairless mouse skin. *Photochem Photobiol* 1999;69:61-70.
  193. Thissen MR, et al. PpIX fluorescence kinetics and increased skin damage after intracutaneous injection of 5-aminolevulinic acid and repeated illumination. *J Invest Dermatol* 2002;118:239-45.

194. Profio AE, Sarnaik J. Fluorescence of HpD for tumor detection and dosimetry in photoradiation therapy. In: Doiron D, editor. Porphyrin localization and treatment of tumors. New York: Alan R. Liss; 1984. p. 301–14.
195. Grossweiner LI. Optical dosimetry in photodynamic therapy. *Lasers Surg Med* 1986;6:462–6.
196. Werkhaven J, Harris DM, Krol G, Hill JH. Light dosimetry in animal models: application to photodynamic therapy in otolaryngology. *Laryngoscope* 1986;96:1058–61.
197. D'Hallewin MA, Baert L. Long-term results of whole bladder wall photodynamic therapy for carcinoma in situ of the bladder. *Urology* 1995;45:763–7.
198. Panjehpour M, Overholt BF, Haydek JM, Lee SG. Results of photodynamic therapy for ablation of dysplasia and early cancer in Barrett's esophagus and effect of oral steroids on stricture formation. *Am J Gastroenterol* 2000;95:2177–84.
199. van Staveren HJ, Beek JF, Keijzer M, Star WM. Integrating sphere effect in whole-bladder-wall photodynamic therapy. 2. The influence of urine at 458, 488, 514 and 630 nm optical irradiation. *Phys Med Biol* 1995;40:1307–15.
200. Marijnissen JP, et al. Pilot study on light dosimetry for endobronchial photodynamic therapy. *Photochem Photobiol* 1993;58:92–9.
201. Wilson BC, Farrell TJ, Patterson MS. An optical fiber-based diffuse reflectance spectrometer for non-invasive investigation of photodynamic sensitizers in vivo. In: Future directions and applications in PDT. Vol. 6. SPIE Inst. Series, 1990. p. 219–32.
202. Wilson BC, Patterson MC, Pogue BW. Instrumentation for in vivo tissue spectroscopy and imaging. *Proc SPIE* 1993;1892:132–47.
203. Bays R, et al. Clinical optical dose measurement for PDT: invasive and non-invasive techniques. *Proc SPIE* 1991;1525:397–408.
204. Bays R, et al. Light dosimetry for photodynamic therapy in the esophagus. *Lasers Surg Med* 1997;20:290–303.
205. Profio AE, Doiron DR. Dose measurements in photodynamic therapy of cancer. *Lasers Surg Med* 1987;7:1–5.
206. Stringer MR, Hudson EJ, Smith MA. The calibration of fiber optic probes used for light dosimetry measurements during photodynamic therapy. *Laser Med Sci* 1995;10:19–24.
207. Vulcan TG, et al. Comparison between isotropic and non-isotropic dosimetry systems during intraperitoneal photodynamic therapy. *Lasers Surg Med* 2000; 26:292–301.
208. Wilson BC, Patterson MS, Lilge L. Implicit and explicit dosimetry in photodynamic therapy: a new paradigm. *Lasers Med Sci* 1997;12:182–99.
209. Johansson T, et al. Feasibility study of a system for combined light dosimetry and interstitial photodynamic treatment of massive tumors. *Appl Opt* 2002;41:1462–8.
210. Lilge L, O'Carroll C, Wilson BC. A solubilization technique for photosensitizer quantification in ex vivo tissue samples. *J Photochem Photobiol B* 1997;39:229–35.
211. Lee CC, Pogue BW, Burke GC, Hoopes PJ. Comparison of photosensitizer (AISPc) quantitation techniques: in situ fluorescence microsampling versus tissue chemical extraction. *Photochem Photobiol* 2001;74:453–60.
212. Andersson-Engels S, Wilson BC. In vivo fluorescence in clinical oncology: fundamentals and practical issues. *J Cell Pharmacol* 1991;3:48–61.
213. Pogue BW, Burke GC. Fiber optic bundle design for quantitative fluorescence measurement from tissue. *Appl Opt* 1998; 37:7429–36.
214. Lee CC, Pogue BW, Burke GC, Hoopes PJ. In vivo spatial heterogeneity and temporal kinetics of photosensitizer (AIPcS2) concentration in murine tumors RIF-1 and MTG-B. *Photochem Photobiol* 2003;2[in press].
215. Glanzmann T, et al. Pharmacokinetics of tetra(m-hydroxyphenyl)chlorin in human plasma and individualized light dosimetry in photodynamic therapy. *Photochem Photobiol* 1998;67:596–602.
216. Moan J. Effect of bleaching of porphyrin sensitizers during photodynamic therapy. *Cancer Lett* 1986;33:45–53.
217. Jacques SL, Joseph R, Gofstein G. How photobleaching affects dosimetry and fluorescence monitoring of PDT in turbid media. *Proc SPIE* 1993;1881:168–79.
218. Ma LW, Moan J, Berg K. Comparison of the photobleaching effect of 3 photosensitizing agents - meso-tetra(m-hydroxyphenyl)chlorin, meso-tetra(m-hydroxyphenyl)porphyrin and photofrin during photodynamic therapy. *Laser Med Sci* 1994;9:127–32.
219. König K, Schneckenburger H, Ruck A, Steiner R. In vivo photoproduct formation during PDT with ALA-induced endogenous porphyrins. *J Photochem Photobiol B* 1993;18:287–90.
220. Ahram M, Cheong WF, Ward K, Kessel D. Photoproduct formation during irradiation of tissues containing protoporphyrin. *J Photochem Photobiol B* 1994;26:203–4.
221. Dickson EFG, Pottier RH. On the role of protoporphyrin-IX photoproducts in photodynamic therapy. *J Photochem Photobiol B* 1995;29:91–3.
222. Moan J, Sommer S. Oxygen dependence of the photosensitizing effect of hematoporphyrin. *Cancer Res* 1985; 45:1608–10.
223. Star WM, et al. Destruction of rat mammary tumor and normal tissue microcirculation by hematoporphyrin derivative photoradiation observed in vivo in sandwich observation chambers. *Cancer Res* 1986;46:2532–40.
224. Henderson BW, Fingar VH. Oxygen limitation of direct tumor cell kill during photodynamic treatment of a murine tumor model. *Photochem Photobiol* 1989;49:299–304.
225. Gibson SL, van der Meid KR, Muran, RS, Hilf R. Increased efficacy of photodynamic therapy of R3230AC mammary adenocarcinoma by intratumoral injection of Photofrin II. *Br J Cancer* 1990;61:553–7.
226. Foster TH, et al. Oxygen consumption and diffusion effects in photodynamic therapy. *Radiat Res* 1991;126:296–303.
227. Foster TH, Gibson SL, Gao L, Hilf R. Analysis of photochemical oxygen consumption effects in photodynamic therapy. *Proc SPIE* 1992;1645:104–14.
228. Sitnik TM, Hampton JA, Henderson BW. Photodynamic therapy reduces tumor oxygenation during and after treatment: effects of fluence rate. *Br J Cancer* 1998;77:1386–94.
229. Veenhuizen RB, Stewart FA. The importance of fluence rate in photodynamic therapy—is there a parallel with ionizing-radiation dose-rate effects. *Radiother Oncol* 1995;37:131–5.
230. Patterson MS, Madsen SJ, Wilson BC. Experimental tests of the feasibility of singlet oxygen luminescence monitoring in vivo during photodynamic therapy. *J Photochem Photobiol B* 1990;5:69–84.
231. Georgakoudi I, Foster TH. Singlet oxygen- versus nonsinglet oxygen-mediated mechanisms of sensitizer photobleaching and their effects on photodynamic dosimetry. *Photochem Photobiol* 1998;67:612–25.
232. Baker A, Kanofsky JR. Quenching of singlet oxygen by biomolecules from J1210 leukemia cells. *Photochem Photobiol* 1992;55:523–8.
233. Niedre M, Patterson MS, Wilson BC. Direct near-infrared luminescence detection of singlet oxygen generated by photodynamic therapy in cells in vitro and tissues in vivo. *Photochem Photobiol* 2002;75:382–91.
234. Timmins GS, Davies MJ. An EPR spin-trapping study of albumin protein radicals formed by the photodynamic action of hematoporphyrin. *J Photochem Photobiol B* 1993;21:167–73.
235. Henderson BW. Probing the effects of photodynamic therapy through in vivo-in vitro methods. In: Kessel D, editor. Photodynamic therapy of neoplastic disease Boca Raton (FL): CRC Press; 1990. p. 169–88.
236. Fingar VH, Mang TS, Henderson BW. Modification of photodynamic therapy-induced hypoxia by fluosol-DA (20%) and carbogen breathing in mice. *Cancer Res* 1988;48:3350–4.
237. Chen Q, et al. Improvement of tumor response by manipulation of tumor oxygenation during photodynamic therapy. *Photochem Photobiol* 2002;76:197–203.
238. Foster TH, Gao L. Dosimetry in photodynamic therapy: oxygen and the critical importance of capillary density. *Radiat Res* 1992;130:379–83.
239. Foster TH, Hartley DF, Nichols MG, Hilf R. Fluence rate effects in photodynamic therapy of multicell tumor spheroids. *Cancer Res* 1993;53:1249–54.
240. Nichols MG, Foster TH. Oxygen diffusion and reaction kinetics in the photodynamic therapy of multicell tumor spheroids. *Phys Med Biol* 1994;39:2161–81.
241. Henning JP, Fournier RL, Hampton JA. A transient mathematical model of oxygen depletion during photodynamic therapy. *Radiat Res* 1995;142:221–6.
242. Hampton JA, Mahama PA, Fournier RL, Henning JP. Photodynamic therapy: computer modeling of diffusion and reaction phenomena. *Proc SPIE* 1996;2675:147–55.
243. Pogue BW, Hasan T. A theoretical examination of light fractionation and dose rate effects in photodynamic therapy. *Radiat Res* 1997;147:551–9.
244. Tromberg BJ, et al. In vivo tumor oxygen tension measurements for the evaluation of the efficiency of photodynamic therapy. *Photochem Photobiol* 1990;52:375–85.
245. Tromberg BJ, et al. Tumor oxygen tension during photodynamic therapy. *J Photochem Photobiol B* 1990;5:121–26.
246. Sitnik TM, Hampton JA, Henderson BW. The effect of fluence rate on tumor and normal tissue responses to photodynamic therapy. *Photochem Photobiol* 1998;67:462–6.
247. Henderson BW, et al. Photofrin photodynamic therapy can significantly deplete or preserve oxygenation in human basal cell carcinomas during treatment, depending on fluence rate. *Cancer Res* 2000;60:525–9.
248. Pogue BW, Braun RD, Lanzen JL, et al. Analysis of the heterogeneity of pO<sub>2</sub> dynamics during photodynamic therapy with verteporfin. *Photochem Photobiol* 2001; 74:700–6.
249. Pogue BW, et al. Tumor pO<sub>2</sub> changes during photodynamic therapy depend upon photosensitizer type and time after injection. *Comp Biochem Physiol A Mol Integr Physiol* 2002;132:172–84.
250. Gibson SL, VanDerMeid KR, Murant RS, et al. Effects of various photoradiation regimens on the antitumor efficacy of photodynamic therapy for R3230AC mammary carcinomas. *Cancer Res* 1990;50:7236–41.
251. Gibson SL, et al. Effects of photodynamic therapy on xenografts of human mesothelioma and rat mammary carcinoma in nude mice. *Br J Cancer* 1994;69:473–81.
252. Gibson SL, Nguyen ML, Foster TH, et al. Efficacy of photodynamic therapy on original and recurrent rat mammary tumors. *Photochem Photobiol* 1995;61:196–9.
253. Foster TH, Gibson SL, Raubertas RF. Response of Photofrin-sensitized mesothelioma xenografts to photodynamic therapy with 514 nm light. *Br J Cancer* 1996;73:933–6.
254. van Geel IP, et al. Vascular perfusion and hypoxic areas in RIF-1 tumours after photodynamic therapy. *Br J Cancer* 1996;73:288–93.
255. Pogue BW, O'Hara JA, Wilmot CJ, et al. Photodynamic therapy of the RIF-1 tumor with verteporfin causes enhanced radiation sensitivity. *Cancer Res* 2003;63[in press].
256. Ehrlich P. Collected studies on immunity. New York: Wiley; 1906.
257. Yarmush ML, et al. Antibody targeted photolysis. *Crit Rev Ther Drug Carrier Syst* 1993;10:197–252.
258. Hasan T, Lin CW, Lin A. Laser-induced selective cytotoxicity using monoclonal antibody-chromophore conjugates. *Prog Clin Biol Res* 1989;288:471–7.
259. Hasan T, Lin A. Monoclonal antibody-chromophore conjugates as selective phototoxins. *J Control Release* 1989.
260. Goff BA, Bamberg M, Hasan T. Photoimmunotherapy of human ovarian carcinoma cells ex vivo. *Cancer Res* 1991;51:4762–7.
261. Jiang FN, Lin CW, Liu G. Development of technology for linking photosensitizers to a model monoclonal antibody. *J Immunol Methods* 1990;134:139–49.
262. Jiang FN, Liu DJ, Neyndorff H. Photodynamic killing of human squamous cell carcinoma cells using a monoclonal antibody-photosensitizer conjugate. *J Natl Cancer Inst* 1991;83:1218–25.
263. Omelyanenko V, Gentry C, Kopeckova P, Kopecek J. HPMA copolymer-anticancer drug-OV-TL16 antibody conjugates. II. Processing in epithelial ovarian carcinoma cells in vitro. *Int J Cancer* 1998;75:600–8.
264. Krinick NL, et al. A polymeric drug delivery system for the simultaneous delivery of drugs activatable by enzymes and/or light. *J Biomater Sci Polym Ed* 1994;5:303–24.
265. Hamblin MR, Miller JL, Hasan T. Effect of charge on the interaction of site-specific photoimmunoconjugates with human ovarian cancer cells. *Cancer Res* 1996; 56:5205–10.
266. Soukos NS, Hamblin MR, Hasan T. The effect of charge on cellular uptake and phototoxicity of polylysine chlorin(e6) conjugates. *Photochem Photobiol* 1997;65:723–9.
267. Rakestraw SL, Tompkins RG, Yarmush DM. Antibody-targeted photolysis: in vitro studies with Sn(IV) chlorin e6 covalently bonded to monoclonal antibodies using a modified dextran carrier. *Proc Natl Acad Sci U S A* 1990;87:4217–21.
268. Goff BA, et al. Photoimmunotherapy and biodistribution with an OC125-chlorin immunoconjugate in an in vivo murine ovarian cancer model. *Br J Cancer* 1994; 70:474–80.
269. Mew D, Wat CK, Towers GH, Levy JG. Photoimmunotherapy: treatment of animal tumors with tumor-specific monoclonal antibody-hematoporphyrin conjugates. *J Immunol* 1983;130:1473–7.
270. Vrouenraets MB, et al. Targeting of a hydrophilic photosensitizer by use of internalizing monoclonal antibodies: a new possibility for use in photodynamic therapy. *Int J Cancer* 2000;88:108–14.
271. Steele JK, et al. Suppressor deletion therapy. Selective elimination of T suppressor cells using a hematoporphyrin-conjugated monoclonal antibody. *Targeted Diagn Ther*

- 1988;1:157–89.
272. Schmidt U, Birngruber R, Hasan T. [Selective occlusion of ocular neovascularization by photodynamic therapy] [German]. *Ophthalmologie* 1992;89:391–4.
273. Schmidt S, Wagner U, Oehr P, Krebs D. [Clinical use of photodynamic therapy in gynecologic tumor patients—antibody-targeted photodynamic laser therapy as a new oncologic treatment procedure] [German]. *Zentralblatt für Gynäkologie* 1992;114:307–11.
274. Popat S, Schmidt S, Schultes B, Krebs D. Photodynamic laser therapy with antibody-targeted staining in an animal model of ovarian cancer. *Arch Gynecol Obstet* 1993;254:440–2.
275. Schmidt S. Antibody-targeted photodynamic therapy. *Hybridoma* 1993;12:539–41.
276. Busch TM, Hahn SM, Evans SM, Koch CJ. Depletion of tumor oxygenation during photodynamic therapy: detection by the hypoxia marker EF3. *Cancer Res* 2000;60:2636–42.
277. Duska LR, Hamblin MR, Miller JL, Hasan T. Combination photodynamic therapy and cisplatin: effects on human ovarian cancer ex vivo. *J Natl Cancer Inst* 1999;91:1557–63.
278. Duska LR, Hamblin MR, Bamberg MP, Hasan T. Biodistribution of charged F(ab')<sub>2</sub> photoimmunoconjugates in a xenograft model of ovarian cancer. *Br J Cancer* 1997;75:837–44.
279. Schmidt-Erfurth U, Diddens H, Birngruber R, Hasan T. Photodynamic targeting of human retinoblastoma cells using covalent low-density lipoprotein conjugates. *Br J Cancer* 1997;75:54–61.
280. Jori G. Factors controlling the selectivity and efficiency of tumor damage in photodynamic therapy. *Lasers Med Sci* 1990;5:115–20.
281. Moan J. Porphyrin photosensitization and phototherapy. *Photochem Photobiol* 1986;43:681–90.
282. Zhou CN, Milanesi C, Jori G. An ultrastructural comparative evaluation of tumors photosensitized by porphyrins administered in aqueous solution, bound to liposomes or to lipoproteins. *Photochem Photobiol* 1988;48:487–92.
283. Maziere JC, et al. Cellular uptake and photosensitizing properties of anticancer porphyrins in cell membranes and low and high density lipoproteins. *J Photochem Photobiol B* 1990;6:61–8.
284. West CM, West DC, Kumar S, Moore JV. A comparison of the sensitivity to photodynamic treatment of endothelial and tumour cells in different proliferative states. *Int J Radiat Biol* 1990;58:145–56.
285. Milanesi C, Zhou C, Biolo R, Jori G. Zn(II)-phthalocyanine as a photodynamic agent for tumours. II. Studies on the mechanism of photosensitized tumour necrosis. *Br J Cancer* 1990;61:846–50.
286. Momma T, Hamblin MR, Wu HC, Hasan T. Photodynamic therapy of orthotopic prostate cancer with benzoporphyrin derivative: local control and distant metastases. *Cancer Res* 1998;58:5425–31.
287. Chen B, et al. Blood flow changes in the RIF-1 tumor in response photodynamic therapy with verteporfin. *Br J Cancer* 2002. [Submitted]
288. McCaughan JS Jr. Photodynamic therapy: a review. *Drugs Aging* 1999;15:49–68.